Fall 12-1-2015

A Platform for Fast Detection of Let-7 Micro RNA Using Polyaniline Fluorescence and Image Analysis Techniques

Partha P. Sengupta
University of Southern Mississippi

A PLATFORM FOR FAST DETECTION OF *LET-7* MICRO RNA USING POLYANILINE FLUORESCENCE AND IMAGE ANALYSIS TECHNIQUES

by

Partha Pratim Sengupta

A Thesis
Submitted to the Graduate School
and the School of Computing
at The University of Southern Mississippi
in Partial Fulfillment of the Requirements
for the Degree of Master of Science

Approved:

_____
Dr. Beddhu Murali, Committee Chair
Associate Professor, School of Computing

_____
Dr. Dia Ali, Committee Member
Professor, School of Computing

_____
Dr. Alex S. Flynt, Committee Member
Assistant Professor, Biological Sciences

_____
Dr. Karen S. Coats
Dean of the Graduate School

December 2015

ABSTRACT

A PLATFORM FOR FAST DETECTION OF *LET-7* MICRO RNA USING POLYANILINE FLUORESCENCE AND IMAGE ANALYSIS TECHNIQUES

by Partha Pratim Sengupta

December 2015

The project describes a new strategy for transducing hybridization events through the modulation of the intrinsic properties of the electroconductive polymer polyaniline (PANI). When DNA-based probes electrostatically interact with PANI, its fluorescence properties are increased, a phenomenon that can be enhanced by UV irradiation. Hybridization of target nucleic acids results in dissociation of probes causing PANI fluorescence to return to basal levels. By monitoring the restoration of base PANI, fluorescence as little as 10^{-11} M (10 pM) of target oligonucleotides could be detected within 15 minutes of hybridization. Detection of complementary oligos was specific, with introduction of a single mismatch failing to form a target-probe duplex that would dissociate from PANI. Furthermore, this approach is robust and is capable of detecting specific RNAs in extracts from animals. This sensor system improves on previously reported strategies by transducing highly specific probe dissociation events through intrinsic properties of a conducting polymer without the need for additional labels. The change caused in fluorescence property of PANI by oligo immobilization and hybridization with mimic *let-7* is measured by fluorescence microscope and the image analyzed by MATLAB. A heuristic algorithm determines color threshold of the fluorescent-active image. This image segmentation helps to determine the average pixel intensity representing the active image foreground of PANI fluorescence triggered by

DNA immobilization and hybridization process. This would help us to quantify response of PANI based biosensor for detecting micro RNA *let-7*.

DEDICATION

For Subhayu and Sreerupa, the two most precious gems of my life.

ACKNOWLEDGMENTS

I would like to express my gratitude to and appreciation for my supervisor, Dr. Beddhu Murali, for his support in joining the Masters in Computer Science program and completing it successfully through rigorous coursework and fruitful research.

I am indebted to my committee member, Dr. Alex S. Flynt, for pushing me to produce stronger scholarship and leading towards a successful culmination of the research work. Without him, it would not have been possible to complete the program.

I would also like to express my sincerest thanks to my other committee member, Dr. Dia Ali, for his excellent advice and support on thesis related topics. Attending Dr. Ali's classes has been additionally helpful.

I am thankful to Miss Crystal McCaffrey for all the support I got from the office of the School of Computing, USM.

I would like to thank Mr. Jared N. Gloria for assisting me in some of my research work related to the thesis.

I would like to thank Dahlia Amato and Doughlas Amato for helping me out in some of the characterization research work.

I would like to thank my lab members, Mosharrof Mondal and Matthew de Cruz, for their valuable suggestion and the discussions we have regarding each other's research efforts.

TABLE OF CONTENTS

LIST OF TABLES

Table

LIST OF ILLUSTRATIONS

Figure

LIST OF ABBREVIATIONS

DNA	Deoxyribonucleic Acid
RNA	Ribonucleic Acid
mRNA	Messenger RNA
AGO	Argonaute
UTR	Untranslated Regions of mRNA
siRNA	Small Interfering RNA
RNAi	RNA Interference
SC	Super Cluster
EDC	1-Ethyl-3-(3-dimethylaminopropyl)carbodimide
PCR	Polymerase Chain Reaction
CP	Conducting Polymer
PNA	Peptide Nucleic Acid
LNA	Locked Nucleic Acid
PANI	Polyaniline
PPy	Polypyrrole
PTh	Polythiophene
PPV	Poly(p-phenylene vinylene)
2D-NMR	2 Dimensional Nuclear Magnetic Resonance
SWNT	Single-Walled Carbon Nanotube
UV	Ultraviolet
FTIR	Fourier Transform Infrared Spectroscopy
DBS	Dodecyl Benzene Sulphonate

PBS	Phosphate-Buffered Saline
*ssDNA*c	Single Stranded DNA Complement
ssDNAm	Single Stranded DNA Mimic
EDS	Energy-Dispersive X-Ray Spectroscopy
Urea-PAGE	Urea Polyacrylamide Gel Electrophoresis
PEG	Polyethylene Glycol

CHAPTER I

INTRODUCTION

Function of Micro RNA

Micro RNAs are small RNA processed from longer transcripts that would fall back on themselves to form hairpin structures. Watson-Crick pairing of A-U, G-C and sometimes, G-U between the two arms of the hairpin form the hairpin structures. Once processed from larger molecules, micro RNA are too small to code proteins, but they play an important role in cells called gene regulation (Ranganathan & Sivasankar, 2014). Gene regulation is a very important process that enables cells different from them. Human body, for example, has many different cell types, all of which contain the same set of genes. Thus, for example, the nerve cells differ from the muscle cells and which are different from the fat cells. This is possible because, some genes are turned off in one type of cells and are turned on in another type of cells and also because of different amount of gene expression in different types of cells. Micro RNAs regulate most of the human genes, and this is important not only for normal cell types but also for diseased cells like cancer cells (Ha, 2011). In animals, there are three key Argonaute proteins (AGO) where ultimately the micro RNAs biogenesis path ends. There are also two endonucleases, Drosha and Dicer, which lead to formation of micro RNAs (MacFarlane & Murphy, 2010). At first, micro RNA is transcribed as a part of larger primary transcript, and then Drosha and its partner Pasha recognize as a part of the hairpin and Drosha cleaves right about one helical turn from the base of the hairpin. This releases the pre micro RNA, which then exits the nuclease. In the cytoplasm, one of the strands of the duplex is loaded into the AGO protein to make the silencing complex. Now, exactly

which strand goes to the silencing complex, and how that happens is a mystery. However, one important clue is that the strand that most likely to go to the duplex is the one which is the least paired at the 5 prime end. In the silencing complex, the micro RNA now directs the AGO to target mRNA and other RNAs. Micro RNA then encounters Dicer, which cuts off the loop, and micro RNA duplex is formed. The biogenesis path of micro RNA is shown in Figure 1.

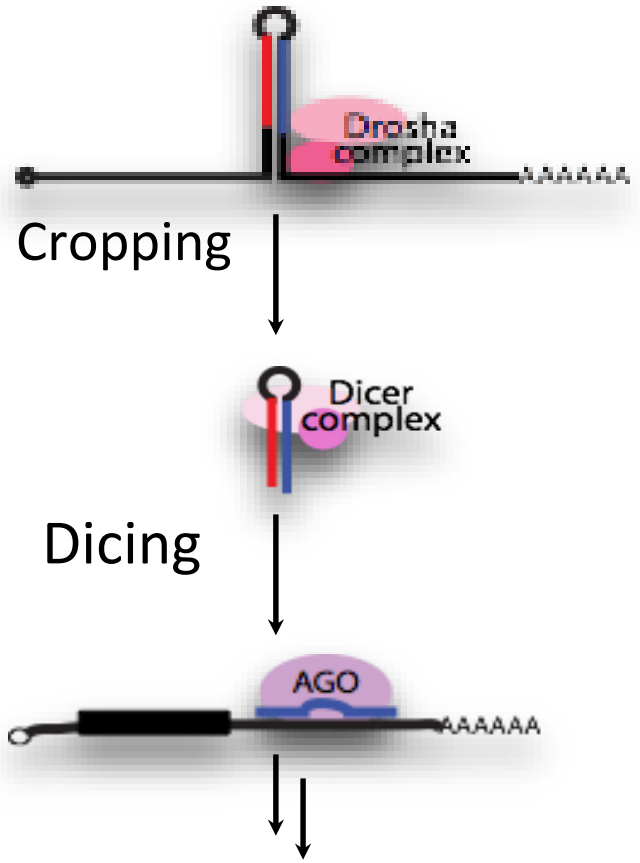

Figure 1. Biogenesis pathway of micro RNA

There are some cases where the processing pathway skips either the Drosha or Dicer step. There is an important micro RNA that is involved in white blood cell development that does not use Dicer for its processing (Mathieu & Ruohola-Baker,

2013). The hairpin goes immediately into AGO which helps it to process into mature micro RNA. There are other classes of micro RNA that manage to bypass the Drosha processing. It is then recognized by Dicer and goes into the pathway. To summarize, the function of micro RNAs, they are small molecules of 21-23 nucleotides in sizes and single stranded. After cleavage of the hairpin structure, the micro RNAs associate themselves with AGO proteins and are then guided to reach the target sites of mRNA. The target sites of mRNA are the 3'untranslated regions (3'UTRs), and the micro RNAs bind at these sites and regulate gene expression which, in turn, are manifested in many biological processes like cell proliferation, apoptosis, immune response, hematopoiesis, insulin secretion etc. (Ekimler & Sahin, 2014; Sevignani, Calin, Siracusa, & Croce, 2006). The micro RNA molecules bind to 3' untranslated regions (3' UTRs) of their target mRNAs.

The first micro RNA was discovered not in humans but instead in model organisms called nematodes, which are often used to study animal development (Bartel, 2004). The first micro RNAs discovered were *lin-4* and *let-7* in 1993. These were found to regulate the developmental stages and their transitions in *C. elegans*. It was concluded that *lin-4* micro RNA down regulates *lin-14* mRNA, and that causes less protein to be made from *lin-14* mRNA. *Let-7* micro RNA was also found in fly, human, and other animals. *Let-7* is expressed at later stages so it might be regulating the time of development along with other micro RNA (Stefani, Chen, Zhao, & Slack, 2015).

Micro RNAs function in two ways: primarily, they have a negative impact on gene expression by causing degradation and translational suppression of mRNA, and they also affect an increase in gene expression. The remarkable conservation of this gene-

silencing mechanism, which is found in most eukaryotes, indicates that it is evolutionarily, ancient, and biologically important. Translation is repressed in mRNA by several ways, for example, (1) by modifying 5'cap in mRNA and (2) by creating proteins which represses translation (Sadava, Hill, Hillis, & Price, 2014). The degradation pathway of mRNA can be studied based on a similar behavior by siRNA, which cleaves mRNA from tenth or eleventh nucleotide. The silencing of mRNA pathway depends on the extent of complement base-airing which inhibit smRNA translational pathway. Many complex eukaryotes also produce small interfering RNAs (siRNAs), which are short (20-25 bp), double-stranded RNAs derived from much longer double-stranded RNA molecules. As in the production of micro RNAs, a protein complex guides these double-stranded siRNA molecules, which are then processed into single-stranded molecules and then each strand pairs with a complementary region on an mRNA. The protein complex then catalyzes the breakdown of the targeted mRNA. These mechanisms for preventing mRNA translation are called RNA interference (Sadava et al., 2014). Micro RNAs and siRNAs are examples of antisense RNA because they bind by base pairing to the "sense" bases on the target mRNAs. siRNAs are target-specific mRNA molecules (from specific genes) because their sequences exactly match the target sequences in the mRNAs. By contrast, micro RNAs do not match their targets perfectly, and therefore each one can reduce the expression of multiple, partially matching genes. RNAi was discovered in the late 1990s, and since then scientists have used synthetic, single-stranded antisense RNAs and double-stranded siRNAs to inhibit the expression of known genes. This technique has been used extensively to block expression of specific genes in the laboratory, as well as in applied situations. For example, macular degeneration is an eye disease that results

in near blindness when blood vessels proliferate in the eye (Quillen, 1999). The signaling molecule that stimulates vessel proliferation is a growth factor. An RNAi-based therapy is being developed to target this growth factor's mRNA, and the therapy shows promise for stopping and even reversing the progress of the disease (Carthew & Sontheimer, 2009).

Many of the micro RNAs are conserved in different species (Hu, Zhu, Zheng, Xiong, & Ding, 2014) for example *miR-1*. It is found in human muscle, heart, and brown fat as well as in fly, and worms. Although the hairpin in *miR-1* differs quite a bit from species to species, the base pairing and the mature micro RNA that is produced are the same across the species. Presumably, this micro RNA *miR-1* was in the last common ancestor of humans, flies, and worms, and presumably, ever since it is playing important roles in the muscle development. Related micro RNAs are also found in inner species. Again using *miR-1* as an example, it can be said that human cells have three different member of *miR-1* family, two of which are identical micro RNA, and the third member is similar at 5' end and have differences in middle and 3' end. The micro RNAs are grouped into families based on the identity of nucleotides 2 through 8, which are critical for target binding (Huang et al., 2015). These families and these micro RNAs are also often conserved. In humans, there are at least 277 genes, which are coding for micro RNA that, are conserved in other mammals (Friedman, Farh, Burge, & Bartel, 2009). There are also hundreds of non-conserved micro RNA genes. Some of them might be playing an important species-specific function in humans especially when they are expressed at higher levels. That is why it cannot be exactly said as how many of them are present, because some of them have been found, but they are expressed at low level to be

detected. So it is unclear what their existence is since they are expressed at low level, and their sequence does not seem to be very important in evolution. One idea is that they are very recently emergent micro RNAs and have not yet found a target (Cheng, Li, & Wang, 2015). It is possible that many of them would disappear before they found a biologically relevant target. Some of these would probably occupy very transiently in evolution without any function, but again, few of them might play important species-specific function, particularly those at higher expression levels (Pak, Rao, Prins, & Mott, 2013). Thus, in a population of RNA, we need to understand the presence of relevant and irrelevant microRNAs which our probes target.

New technologies being developed and used to determine and predict the attachment of micro RNA on target sites on mRNA. One of them is the thermodynamic experimentation to determine energy required for favorability in hybridization of micro RNA and target mRNA and favorability of primary and secondary structure formed during hybridization. Another approach is the use of bioinformatics and related algorithms, which compute the possible complementarity of micro RNA and target mRNA interactions (Ekimler & Sahin, 2014). Computational methods help to determine the potential target sites on 3'UTR regions of mRNA and Watson-Crick complement of the micro RNA. These seed regions are then analyzed for thermodynamic favorability of duplex structure (Xu, Lucas, Wang, & Liu, 2014). .

Micro RNAs as Biomarkers and Imaging Method

Micro RNAs are molecules which have important roles in physiological processes which lead to diseases like cancer, sepsis, and autoimmune disorder (Zhao et al., 2012). Micro RNAs are thus important biomarkers whose concentration in serum is

an important indicator of different disease states. Oncogenes which have mutations, genes which suppress tumor, and genes which repair mismatch serve as micro RNA biomarker (Kwon & Shin, 2011). It is important to detect snapshots of micro RNA to understand cancer staging in early stages. Since survival of cancer patients is very much dependent on detection of cancer at an early stage, detection of micro RNAs may provide an important clue for cancer detection at an incipient stage and thus its possible cure (Debnath, Prasad, & Bisen, 2010). Among potential micro RNA cancer biomarkers, *let-7* seems the most useful one (Shell et al., 2007). This micro RNA is expressed in most tissues and is responsible for maintaining differentiation. In mammals, this appears to be a consequence of targeting HMG2A, K-Ras, and c-Myc (Johnson et al., 2005; Lee & Dutta, 2007; Sampson et al., 2007; Ross et al., 2000). Based on gene expression profiles, cancer cell lines can be segregated into two groups: super cluster 1(SC1) which consists of undifferentiated cells that possesses a more mesenchymal-like fate, and super cluster 2 (SC2) which is composed of more differentiated cells (Algeciras-Schimnich et al., 2003; Boyerinas, Park, Hau, Murmann, & Peter, 2010). Tumor cells exhibiting a SC1 signature are associated with poorer prognosis. The biomarkers E-cadherin and vimentin can be used to distinguish SC1 and SC2 cells (Algeciras-Schimnich et al., 2003; Boyerinas et al., 2010). More recently, a study suggested that loss of *let-7* expression is a better indicator of cancer phenotype than these protein markers (Shell et al., 2007). Additional studies have shown that loss of *let-7* expression is a common phenomenon in high-grade tumors (Boyerinas et al., 2010). Compatibility with pathology practices is an important consideration for widespread adoption of a particular biomarker (Henry & Hayes, 2012). The standard of care in diagnosis of solid tumors revolves around pathological

examination of cell morphologies in biopsies. Ideally, opinions of a pathologist are combined with assessment of cellular genetics to give the most complete picture for diagnosis. Immunohistochemical techniques are frequently employed to this end (E-cadherin, vimentien, etc.); however, they require several days to complete and are limited by antibody availability and quality. Detection of RNAs via in situ hybridization is more complicated requiring antisense probes in addition to antibodies. Critically, both of these techniques are too lengthy for intra-operative consultation. While micro RNAs, particularly *let-7*, are attractive biomarkers for cancer phenotype, there are significant barriers to their use in a clinical setting. Most methods rely on extracted RNAs, which would require destruction of biopsy samples making them unavailable for re-examination. Using RNA isolated en masse from a tissue may also miss genetic changes that have taken place in tumor cell subpopulations. While it is possible to assess micro RNA expression in individual cells of a tissue using in situ hybridization, there is need for exotic locked nucleic acid (LNA) probes and special fixation techniques that involve the use of 1-Ethyl-3-(3-dimethylaminopropyl)carbodimide (EDC) (Mestdagh et al., 2009; Iorio & Croce, 2012). This would require modification of existing tissue processing regimes. Thus, a new strategy to localize changes in Micro RNA expression in tissue biopsies will be a welcome armament in the battle against cancer. Biochip is synonymous to the word computer chip and can have printed circuits on silicon wafer. However, the term more precisely defines surfaces having spots made of probes, which can capture corresponding targets. Thus, by designing the position of microscopic spots with specific probes, the target sequence can be quantitatively detected. The probe can be single-stranded DNA, protein, or antibody. Typically, a drop of target sample is added to the

bio-chip and the corresponding target signature is identified within 15 min. Figure 2 shows the different possible applications of a biochip in point-of care diagnosis.

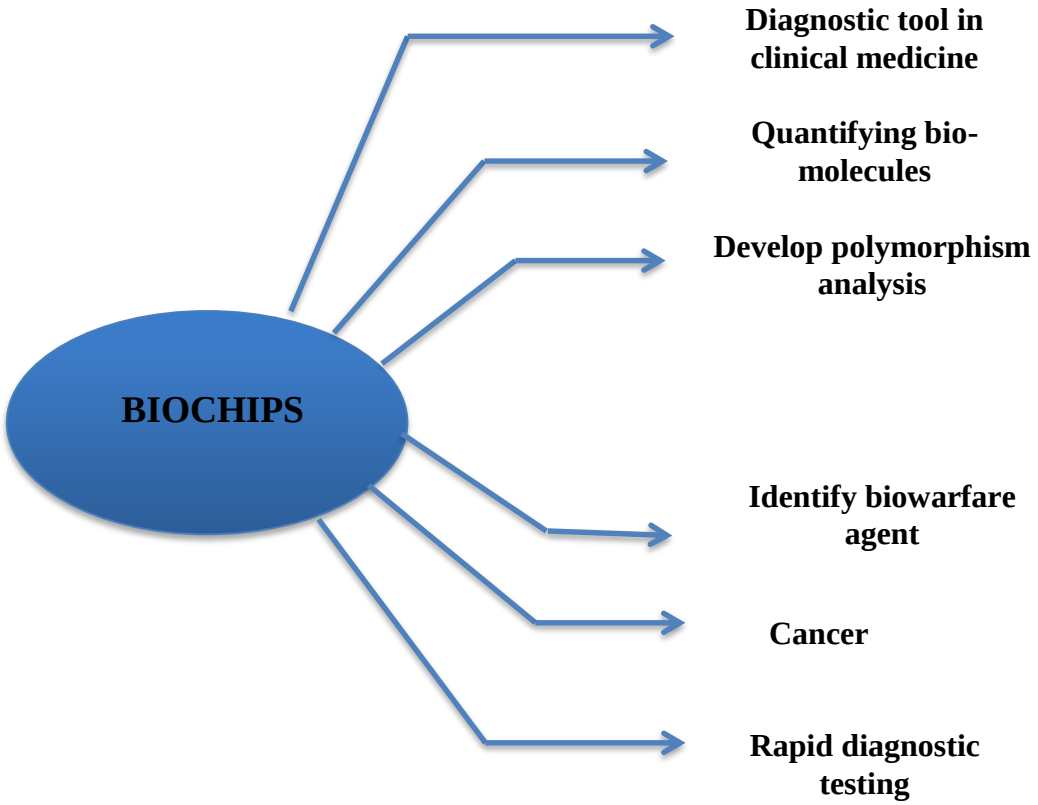

Figure 2. Point-of care application of a biochip

The hybridization between two DNA or a DNA-micro RNA depends on the complementary base pairs and string hydrogen bonds between nucleotide bases (Lodish, Berk, Zipursky, Matsudaira, Baltimore and Darnell, 2000). Higher levels of hybridization results in higher levels of compact Watson-Crick base pairing with strong hydrogen bonds between two strands. Figure 3 shows hybridization between two complementary strands on a substrate of a biochip.

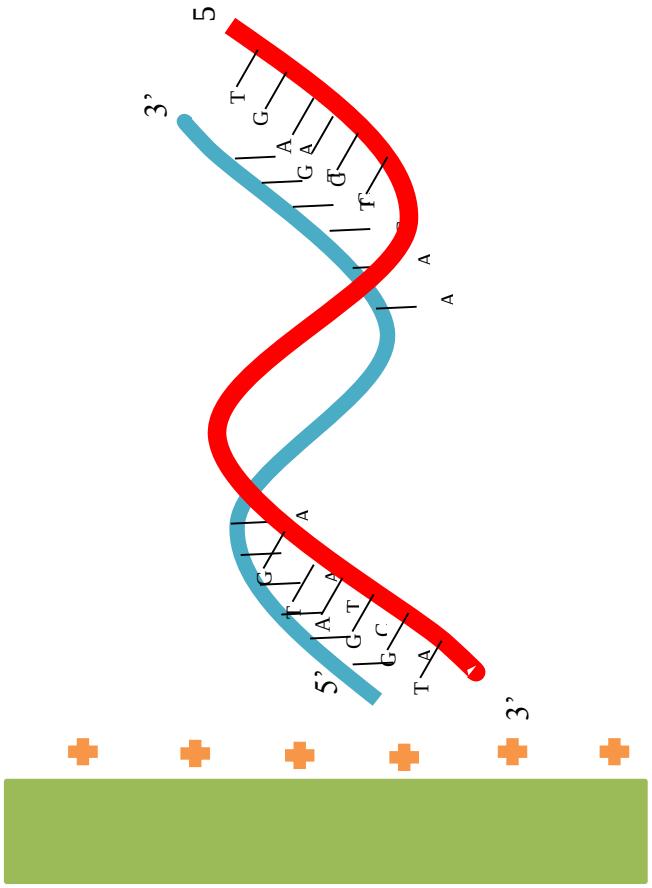

Figure 3. Hybridization of complementary DNA strand on substrate of biochip

In a biochip, there is an array of spots that contain the probes which have been selected to specifically bind with the target oligonucleotide sequence. This binding occurs when the bio-chip is exposed to solution containing the target. As a result, the probes are no longer attached to the biochip. After washing of any unbounded or loosely bound strands, fluorescence measurements are conducted. The fluorescence intensity is directly related to the amount of target sequence present in the analyte. The hybridization condition, particularly temperature, is also normalized such that under the condition the target nucleotide is strongly bound with the probe, and non-specific bindings are washed off by the washing procedure. Fabrication of biochips could involve (1) fine pins printed

with probes on glass slides, (2) inkjet printing of probes on the substrate, and (3) photolithography with masks etc. (Buxbiom et al., 2007; Lee et al., 2006). Biochips typically consist of spotted microarrays where small DNA single strands mostly PCR products, are spotted on the glass surface in formation of a grid. Sometimes, for accurate grid spacing, robotic arms are used, which dip fine pins or needle in a wells containing DNA probes and deposit each probe at a fixed position in the grid. This type of fabrication of biochips can be customized by research scientists through the selection of probes for specific target nucleotide sequences of interest. This allows for considerable flexibility in labeling and measurement techniques when compared with buying costly commercially available microarrays containing probes that are not of research scientist's interest (Schirwitz et al., 2012). The substrate used is usually glass or silicon chip, and the probes are fixed on surface by surface engineering techniques on the probes such as attachment of reactive functional groups. The covalent bonding between probes and the substrate are due to epoxy-silane or amino-silane bondings between the reactive functional groups attached to the probes and the substrate (Thamizhvanan, Kumuda, & Nandakishore, 2012; Adessi et al., 2000). The analysis of micro RNA pattern in a biochip is further quantified with supervised algorithms such as double hierarchical clustering methods resulting in color clustered image maps (Rao, Benito, & Fischer, 2013). These analyses have already provided increased prognostic capability and led to novel, early stage discovery of various types of cancer. This probabilistic mapping is a simple and powerful method to determine average distributions of visualized objects. Clustering is a kind of unsupervised learning based on distances between each data point. Similarities between microscopic images can be evaluated using clustering with appropriate image

metrics (Dima et al., 2011). Image segmentation can be done on the basis of pixel intensity (Singh & Singh, 2010). The goal of image representation is to partition a given image in such a way that the extracted image is easier to analyze. Image segmentation locates the pixel intensity of the object and also lines, curves, and boundaries surrounding the object. It is based on differentiating image on basis of some common characteristics (Abubakar, 2012). Edge detection is a mathematical tool, which segregates the boundary of the object with the surrounding background based on change of pixel intensity (Singh & Datar, 2013). The boundary, which has a sharp change of pixel brightness, is considered an edge (Shapiro & Stockman, 2001). Edge detection is a basic requirement in several images processing applications.

In the present work, preliminary analysis was first performed using a very simple image processing technique, using a single threshold for the entire image. The input image came from a locally fabricated biochip, where an image is obtained after probe-target interaction. However, since the image had a non-uniform pixel intensity distribution, a single threshold was unable to extract the features of the image. A better way of normalization of pixel intensity is to put them in logarithmic scale (Fouad, Mabrouk, & Sharawy, 2014). The bounding boxes of each pixel obtained from individual region properties can be used to apply single threshold values to each spot for better analysis. All this information is integrated with a database and matching with calibrated data is being done to detect rapidly and accurately micro RNAs as biomarkers of specific cancer phenotypes.

Conducting Polymers as Sensing Element

Conducting polymers (CPs) are a class of specialty polymers with long conjugation length allowing flow of electrons like metals. This unique electron conjugation in conducting polymers results in characteristic physical and chemical properties such as the electrical conductivity, electron affinity, and ionization potentials. A mechanism called Peierls distortion localizes this electron conjugation of labile π bonds in ground state (Travas-Sejdic, Aydemir, Kannan, Williams, & Malmstrom, 2013). Doping process causes excitement of these π electrons to excited levels called π* states and these π-π* transitions are also localized causing important electronic states which help to understand the underlying mechanisms of conduction and optical properties of CPs such as polarons, bipolarons, and solitons (Peng, Zhang, Soeller, & Travas-Sejdic, 2009). The π-π* transition representing band gap of CPs is its intrinsic property dependent on the structure and flow of electrons in a conjugated path. However, this electronic structure of CPs is sensitive to local change in the environment especially through physical and chemical bonds with the environment that could cause a change of optoelectronic properties of CPs. Such a perturbation of the electronic bonding environment can be caused by the DNA immobilization of the probes or the subsequent possible hybridization of the immobilized probe with target. Such changes in electrical and optical properties of CPs in presence of biological recognition element can be used for its interrogation (Gawel, Barriet, Sletmoen, & Torger-Stokke, 2010). Thus, CPs can possibly be used as important transduction element for nucleic acid biosensors. The configuration of a biosensor, or typically, a biochip involves CPs as transduction probes immobilized with single stranded DNA probe. The probe can also involve peptide nucleic

acid (PNA) or locked nucleic acid (LNA), which has added functionality and performance characteristics over single stranded DNA probe. The probe has nucleotide base sequences that are complementary sequence to the target analyte. The base pairing creates signature images, which are analyzed by image processing software and able to detect the micro RNAs responsible for particular disease states (Abu-Salah et al., 2015). The interaction of probe and target is transduced to the CP-electrolyte layer and this changes the local environment of conjugated structure of CPs causing changes in electrical and optical properties. Thus, the orientation of the DNA probe and conformational requirement of attachment with target nucleotide sequence arei important for signal transduction (Zhang et al., 2011a). The type of immobilization of the probe with CPs also plays an important role in creating the base value on which the hybridization event is detected. There are different methods of immobilization as covalent attachment, electrostatic bonding, or affinity-based attachment depending on the design requirement of creating a biochip (Zhang et al., 2011a; Rahman, Li, Lopa, Ahn, & Lee, 2015). The choice of the transduction element plays an important role for proper signal capture in terms of change in electrical or optical properties of CPs (Rahman et al., 2015). The most researched CPs as shown in Figure 4, for development of nucleic acid sensor are polyanilne (PANI), polypyrrole (PPy), polythiophene (PTh) and poly(phenylene vinylyene) (PPV). However, there is enough scope of research with these polymers in optimizing fabrication of CP coating, immobilization of probe and hybridization of target sequence. Finally detection techniques and developing algorithms for image analysis would enable to develop a fast, robust and accurate sensor.

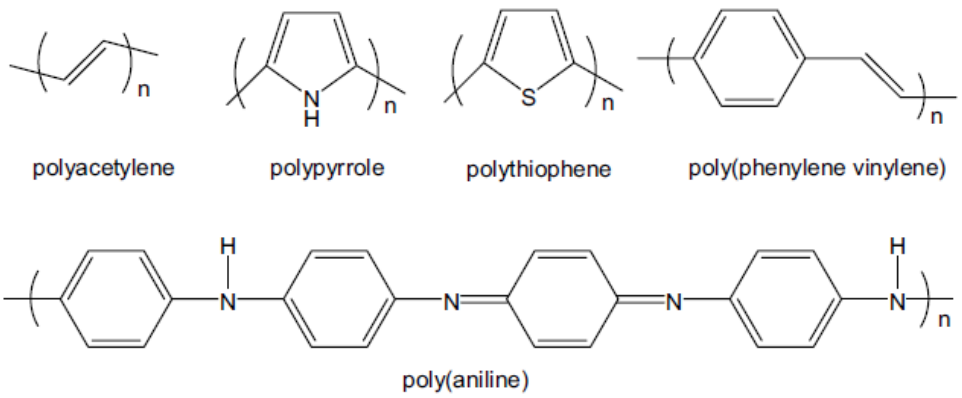

Figure 4. Common conducting polymer

Conducting polymers can be produced by template synthesis method, using pores in a micro porous membrane as a template for nanoscale fibers or wire formation (Pan et al., 2010). DNA or peptide nucleic acid templating generates a nanowire width, which has very small structures. A one-pot synthesis of conducting polymer monomer like aniline, pyrrole or thiophene in presence of probe oligo along with all other reaction ingredients and buffer solution can be done at room temperature (RT) condition. The reaction solution is then drop coated on an interdigitated microelectrode chip. The target micro RNA was cast on the electrode for RT hybridization. The signal measurement is a simple and straightforward linear relationship between the conductance and micro RNA concentration measured by an electrochemical analyzer (femtogram level). The nanowire CPs on probe oligo template are usually very robust at different environmental conditions. The specificity of the biosensor depends on choice of probe oligo for effective hybridization of target micro RNA and also effective signal transduction of CPs. For effective interaction, copolymerization of CPs for nanowire synthesis on PNA template can be done (Hahm, 2011). The hybridized probe oligo and target micro RNA results in a negatively charged surface originating from the phosphate groups in the micro RNA

(Zhang, Chua, Chee, Agarwal, & Wong, 2009). The negatively charged surface polarizes high proton/ionic concentration and a local environment of high acidity, which results in doping of conducting polymer and higher conductance (Song & Choi, 2013). The more micro RNAs are hybridized, the more is the conductance of the sensor. In-situ synthesis of conducting polymer, nanowire on peptide nucleic acid (PNA) template during hybridization with target micro RNA can also be done (Chen et al., 2010). This reaction scheme requires PNA and conducting polymer monomer during the target micro RNA hybridization process. The local acidic environment during hybridization would initiate polymerization of monomer to form polymeric nanowires (Park, Kwon, Lee, Jang, & Yoon, 2014). The higher deposition of in-situ conducting polymer nanowire deposition would result in higher conductance. This method would develop a highly sensitive biosensor chip for micro RNA detection. Another method is noncovalent wrapping of carbon nanotube by PNA for fluorescent-based detection of biosensor chip for hybridization with target micro RNA (Star et al., 2006). This noncovalent attachment of carbon nanotube on PNA probe still preserves the intrinsic property of carbon nanotube which acts as transduction element. The fluorescence property of SWNT is quenched by energy transfer from PNA and carbon nanotube. The noncovalent functional molecules were deposited in a microelectrode, and the fluorescence spectrum was measured in presence of hybridized target micro RNA. There are lots of potential experimental opportunities to construct a sensor technology for micro RNA expression using conducting polymers and ssDNA oligos (Garzon, Mareucci, & Croce, 2010). To deliver the most viable technology platform, an exploration of the properties of sensors using alternate conducting polymer and oligo chemistries is necessary. Thus, there is a need to

synthesize additional conducting polymers like PPy and PTh, and their copolymers to test the signal transducers or micro RNA hybridization to sensor properties. In conjunction with these alternate conducting polymers, there is a need to test the suitability of the use of different oligo chemistries in sensor construction, as shown in Table 1.

Table 1

Alternate Conducting Polymer and Oligo Chemistries. Left column lists the different CPs that will be tested for their association with oligo probes. Right column lists the oligos

Transducer CPS	Oligonucleotides
1. Polyaniline (PANI)	Single-stranded DNA (ssDNA)
2. Polypyrrole (PPy)	Single-stranded RNA (ssRNA)
3. Polythiophene (PTh)	Peptide nucleic acid (PNA)
4. Poly(aniline-co-thiophene)	Lock nucleic acid (LNA)
5. Poly(pyrrole-co-thiophene)	Morpholino
6. Poly(aniline-co-pyrrole)	
7. Poly(aniline-co-pyrrole-co-thiophene)	

Using different characteristic measurements, the conducting polymers and oligonucleotides can be investigated as viable sensors. PANI has intermediate conductance properties relative to PPy and PTh. The five-member heterocyclic repeating

units of PPy have low resonance energy and higher localization of positive charge on nitrogen. This would cause higher sensitivity of PPy on oligo immobilization, compared to PANI (Bai & Shi, 2007). PTh has sulphur as a heteroatom, instead of the nitrogen in PANI and PTh. Sulphur is less hard basic than nitrogen, and the high resonance energy of thiophene subunits and low basicity of sulphur would cause higher stability of sensor response (less noise) in PTh (Ates, 2013). Changes in the properties of conducting polymers arising from different heteroatoms and ring structures would affect their interactions with oligos and impact selectivity, sensitivity, and stability of the sensor. There is also a need to test different conducting copolymer varieties. The block copolymers of aniline-co-pyrrole, aniline-co-thiophene and thiophene-co-pyrrole, and terpolymer of aniline-co-pyrrole-co-thiophene by microemulsion polymerization are synthesized using varied co-monomer composition to modulate their morphology, and their electrical, electrochemical, and optical properties. These copolymer varieties would be bound with oligos, as shown in Table 1, and investigated for alterations in their conductance. The block copolymer derived from conducting polymers has different morphologies, and their properties depend significantly on the characteristics of particular block polymeric segments. For example, a higher ratio of co-PPy in the copolymer structure would lead to higher sensitivity, while the characteristics of co-PTh would result in more stable sensor response. A significant ratio of co-PANI would result in intermediate properties with respect to co-PPy and co-PTh. Ultimately, each co-polymer can be tested for their capacity to detect hybridization between probes and complementary oligos. The lists of oligos that can be tested are shown in Table 1 as single stranded RNA, PNA, LNA, and morpholinos. PNA does not have a negatively

charged phosphate group to interact with a CP, however, it may do so through its polar carbonyl group. Some reports have suggested that PNA shows higher specificity and binding strength in PNA-micro RNA complexes. Another oligo to be used as probes is locked nucleic acid (LNA), which is designed for increased sensitivity and specificity (Koshkin et al., 1998). The negatively charged phosphate group of LNA would associate with positively charged CPS. LNA may show higher affinity for CPS due to its compact, bridged conformation. Another oligo chemistry that can be tested for micro RNA sensing is morpholinos. In the morpholino backbone, the polarization of phosphorodiamidate groups might cause steric inhibition and poor bonding with conducting polymers, which may make them better candidates for our probe dissociation-based sensor. The non-ionic bonding groups present in morpholino would also enhance specificity during hybridization with target micro RNA. Understanding the supramolecular chemistry of the oligos bound to conducting polymers requires sensitive analytical techniques. An AVIV UV-Vis spectrophotometer can be used to measure conducting polymer-oligo interaction in terms of absorption properties of conducting polymers and oligo nucleotides. The hypochromic effect, which arises due to conducting polymer-oligo interaction, would help to identify superior combination of oligo and conducting polymer. The melting temperature, which corresponds to the inflection point in the absorbance-temperature plot, can quantitatively measure the type of interaction of conducting polymer and ologos. Conducting polymer-oligo interaction can be investigated by 2D-NMR and polarized light spectroscopy. The chemical shift of the ^{1}H-NMR of oligos and that of the ^{31}P-NMR of DNA will likely be sensitive to conformational changes of oligos upon binding to CPs. 2D-NMR will provide structural and dynamic information concerning the

CP-oligo complexes. It would provide insight on the conformational changes of oligos interacting with polymer varieties described above. Polarized light spectroscopy can be used to investigate the nature of the non-covalent binding between conducting polymers and oligos, and provide a quantitative measurement of conducting polymer-oligo interactions to help identify a suitable combination of the sensor technology.

Research Objectives

An important research question we face is, how to analyze micro RNA, which is an important molecule and acts as biomarkers in a sequence of biological steps leading to dreadful diseases like cancer? Micro RNAs are of small size, which greatly complicates the use of standard molecular biology methods like PCR, and hybridization-based arrays that depend on melting temperature normalization and binding dynamics of complementary probes. There is a need to detect these small-sized and potentially baffling evolutionary micro RNAs by a rapid, sensitive, and robust sensor platform and also scale it to multiplex analysis for specific and accurate detection of multiple micro RNAs responsible for a disease state. On this background, we propose a nanomaterial-based sensor, using intrinsic property of conducting polymer PANI. The choice of PANI was based on a compromise of properties like sensitivity and stability compared to other CPs like PPy and PTh substitutes. To avoid selection of probes- specific target micro RNA based on hybridization, we rely on electrostatic interaction between PANI and probe immobilization rather than covalent attachment. The former gives flexibility to sensor response and would markedly increase the sensitivity of the response. Moreover, measuring intrinsic property of PANI avoids a pivotal step in conventional molecular biology as direct or indirect labeling of micro RNAs. Labeling affects both the stability

and sensitivity, and a sensor based on intrinsic property of CPs has a better chance of success in microarray analyses. CPs is sensitive to alteration of local environment like nucleotide probe immobilization and can effectively transduce the changes in biological events around them. The conjugated electronic structure is highly sensitive to any electron affinity and conformation-based events which affect its electron flow by causing change in torsional angle, planarity of benzene rings, inter-chain interaction and modifying its intrinsic property like fluorescence spectra and quantum yield. Another reason for the choice of measuring fluorescence property of PANI is that fluorescence measurement is a principal tool to make observation for cellular analysis. Finally, we would use image processing as a powerful detection tool of micro RNAs to couple microscopy technique and signal processing.

CHAPTER II

UTILIZING INTRINSIC PROPERTIES OF POLYANILINE TO DETECT NUCLEIC ACID HYBRIDIZATION THROUGH ELECTROSTATIC INTERACTION

Introduction

Conductive polymers (CPs) have many applications in electronic devices and molecular sensors (Janata & Josowicz, 2003; Saranya, Rameez, & Suramania, 2015; Ates, Karazehir, & Sarac, 2012; Yoon, 2013; Gerard, Chaubey, & Malhotra, 2002; Falcao, & de Azevedo, 2002). In biosensors, a promising use of CPs is in the sensing of nucleic acids: a versatile strategy for characterizing cells and their behaviors (Travas-Sejdic et al., 2014; Lou, He, Okelo, & He, 2006). The greatest challenge to use CPs is their low solubility and poor mechanical properties leading to abysmal processability for usage. To overcome these problems, there have been several novel methods like using long chain organic dopants (Singu & Palaniappan, 2013), functionalization of monomer ring (Feldman & Martin, 2012), or preparations of composites (Sabirmeeza & Subhashini, 2013). Introduction of long chain organic dopants with sulfonic acid groups onto the backbone of CPs allows aqueous dispersion, which is an important criterion for in-phase interaction with water-soluble nucleotides.

There have been many reports of incorporating CPs into hybridization-based RNA/DNA sensors (Rahman et al., 2015; Peng, Zhang, Soeller, & Travas-Sejdic, 2009). The predominant strategy involves covalent attachment of probes via crosslinking or entrapment in CP matrices during polymerization (Rahman et al., 2015; Peng et al., 2005; Gaylord, Heeger, & Bazan, 2003). There are also reports of exploiting the ability of CPs to form electrostatic complexes with probes through interaction of positively-charged π-

CPs and negatively-charged nucleic acids (Preat et al., 2011). Electrostatic attachment of probes to CPs eschews multiple reaction steps for immobilizing probes, making fabrication straightforward. Studies using this strategy report high specificity, where even a single base-pair mismatch is easily detected, providing higher specificity compared to platforms that utilize permanent probe attachment (Zhang et al., 2011).

The goal of this work is to develop a sensor platform based on electrostatical probe attachment that, unlike other reports, exploits the intrinsic property of a CP (Wolfbeis, 2015). There are many CPs that could comprise viable sensor technologies; however, here the focus will be on PANI. The chemical structure of PANI and the facile method of assembly make it compatible with many chemistries found in nature (Velusamy et al., 2011). The conjugated π electron backbone of PANI leads to high electrical conductivity, low ionization potential, high electronic affinities, and optical properties that can be used for quantification of biochemical events (Preat et al., 2011; Liu, Tian, Tiefenauer, Nielsen, & Knoll, 2005). PANI is also able to form electrostatic bonds with nucleic acids, and has been used in DNA/RNA sensors (Ahuja, Mir, & Kumar, 2007; Santhanam, 1998; Skotheim, Elsenbaumer, & Reynolds, 1998). The single most important characteristic property of PANI and also of most CPs is their delocalized electronic structure. The localized positive charges on this conjugated structure are also mobile, leading to a larger number of interactions with fixed negative charges, as in nucleic acids, than substrates with immobile positive charges (Santiago, Pereira, & Bulhoes, 1998; Sambasevam, Mohammad, & Phang, 2015).

Positively-charged, doped PANI exhibits low fluorescence, but upon association with negatively-charged molecules, it acquires high-energy electrons causing increased

fluorescence emission levels (Raymond et al., 2005). Thus, negatively charged molecules like DNA, by associating with PANI, can un-dope it, causing higher fluorescence intensity. Such interactions alter chain organization of conducting polymers by changing torsional angle of conjugated rings and inter-chain interactions (Noriega et al., 2013), which can affect both optoelectronic properties like fluorescence and electrochemical properties like resistance of CPs (Darling, 2008). Thus, interactions demonstrated to alter one property can be expected to affect other properties. The approach described here uses UV irradiation to enhance interaction between probe oligonucleotides and PANI. This allows interactions of the CP with probes to be distinguished from non-specific interactions with other molecules.

The sensor developed around these interactions is a sensitive and specific platform for detecting oligonucleotide interactions, and this sensor is capable of detecting expression of micro RNAs in total RNA extractions from *Drosophila Melanogaster* (Fruit Flies). This class of small regulatory RNAs has a great potential as biomarkers for numerous diseases, and due to their small size, these RNAs are ideal molecules for detection with this method. Specifically, the sensor was developed to detect the micro RNA species, *let-7*. This gene is present in all animals, and has critical roles in tissue homeostasis (Shell et al., 2007). The capacity of the sensor to detect these molecules validates its ability to detect specific nucleic acids in complex biological samples.

Experimental

Materials

Aniline and ammonium peroxydisulfate were purchased from Fisher Scientific, USA. Sodium dodecylbenzene sulfonate (Na-DBS) was purchased form Pfaltz and

Bauer, USA. Chloroform was obtained from EMD Chemicals, USA. All the reagents were analytical grade and are used without purification. Water used in all measurement and solutions was DNase/RNase free distilled water. DNA primers were obtained from Eurofins MWG Operon, USA. DNA sequences are:

-probe (antisense to *let-7*) 5' ACTATACAACCTACTACCTCA-3'

-complementary (identical to *let-7*) 5'-TGAGGTAGTAGGTTGTATAGT-3'

-mis-match (One base mismatch) TGAGGTAGTAAGTTGTATAGT

-unrelated oligo, 5'-TAATACGACTCACAGGGAGACCCAAG-3'

Phosphate-buffered saline (PBS) was made using pre-formulated tablets (Fisher Scientific). Urea- polyacrylamide gels were made using the UreaGel system from national diagnostics. Total RNA extraction reagents used the TRI-reagent method (MRC).

Processable PANI Synthesis

Aniline (1 mL, 11 mmol) was completely dissolved in 60 ml of chloroform in a 250 mL round bottom flask, and the solution was stirred at 600 rpm and cooled to 0 °C. Na-DBS (7.44g, 21 mmol) was added into the aniline solution and stirred vigorously at 0-5 °C. APS (3.072 g, 13.5 mmol,) was dissolved in 20 mL water in a beaker and is added drop wise into the reaction mixture for 30 min to avoid overheating of the reaction mixture. The reaction mixture was stirred at 0-5 °C for 24 h and is allowed to reach room temperature for 24 h. The reaction mixture initially turned to milky white, then dark brown, and finally into a dark green colored PANI-DBS dispersion in chloroform-water mixture. The resultant PANI-DBS solution was filtered in a Buchner funnel, and then the solution is mixed with 80 mL chloroform and 120 mL water in a separation funnel. The

solution stood for 24 h after which the dark green PANI was collected from the separation funnel, while unreacted DBS and APS were left in the aqueous supernatant.

Characterization of Synthesized PANI

The synthesized PANI solution was drop coated onto a clean 2″x 2″ silicon wafer and dried at 40 °C for 48 h in an oven. The PANI-coated silicon wafer was analyzed *via* FT–IR with a Thermoscientific Nicolet 8700 with g-ATR (Attenuated Total Reflectance) attachment. The sample was analyzed with 128 scans. The PANI solution was diluted 20x with water in which, 200 µL of the diluted solution was added into a 96 well polypropylene microplate for UV spectroscopy. The UV absorbance of the PANI solution in the microplate was measured with a Spectramax M3, Molecular Devices, in the range 350-850 nm. Dynamic Light Scattering (DLS) measures the size and distribution of the nanoparticles using a Microtrac Nanotrac Ultra NPA150. Microtrac Flex software (v.10.6.1) employs non-negatively constrained least squares (NNLS) and cumulants analysis to obtain the intensity –weighted "z-average" mean particle size as the first cumulant, and the polydispersity index from the second cumulant measures the particle size and distribution of the synthesized PANI dispersed in water. High-resolution field emission SEM (FE-SEM) was imaged with Zeiss Sigma Variable Pressure, Field Emission Gun Scanning Electron Microscope at 10 kV in high vacuum mode with Thermo energy dispersive and wavelength dispersive X-ray detectors (EDS/WDS) at an accelerating voltage of 20 kV. Samples were sputter coated with silver at instrument and reported thickness of the coating is 5 nm.

PANI- Probe Mixing and UV Irradiation

The synthesized PANI had a solid content of 0.12 g/mL. 200 µL of PANI solutions diluted 10X (~2400 µg) or 100X (~240 µg) were mixed with different concentrations of probe ssDNA oligos by gentle rocking for 15 min. Most experiments used 2400 µg of PANI and 0.08 µg of probe. The solution was UV irradiated at 100 $\mu J/cm^2$ for different time intervals. PANI-probe complexes were pelleted by centrifugation at 13,300 rpm for 5 min and resuspended in water.

Emission and Excitation Steady State Fluorescence Measurement

PANI-probe mixtures were added into a 96 well microplate and emission fluorescence was measured in the range 270-850 nm by excitation at 250 nm in a Spectramax M3, Molecular Devices, with an emission peak around 500 nm. The excitation fluorescence intensity was measured by excitation at 350 nm and two peaks were observed for PANI, a high intensity peak at 350 nm and a lower peak at 700 nm. This procedure was also performed for probe-complexed–UV treated PANI.

Hybridization of PANI-probes with Complementary Oligos and Total RNA Extracted from Drosophila

Oligos or total RNA isolated from *Drosophila melanogaster* were added to UV-treated PANI-probe complexes in PBS and incubated @ 37 °C for 15 min by gentle rocking. The solution was pelleted by centrifugation at 13,300 rpm for 5 min, washed twice with PBS, and re-suspended with water. A Spectramax M3, Molecular Devices, was used to measure fluorescence.

Fluorescence Microscopy Measurement of Hybridized Duplex

PANI was drop coated on borosilicate glass coverslip and dried in oven at 40 °C for 48 h. Probe (8 µg) was added on dried PANI film and irradiated with UV light (100 µJ/cm^2) for 1200 ms. The PANI-probe film was washed with 0.01 M PBS and dried at 40 °C for 48 h. Hybridization was subsequently performed for 15 mins by adding 8 µg of oligos complementary to the probe coated on PANI. Fluorescent images were obtained using a Leica DMIL at 40X magnification, with a 488nm long pass filter.

Urea-polyacrylamide gel electrophoresis

The fluorescein-tagged probe (8 µg, Fprobe) was mixed and attached *via* UV with 200 µL (~2400 µg) of PANI. Hybridization was performed as described above, and the PBS wash was collected. Wash solution containing any dissociated oligos (15 µL) was separated by electrophoresis on a urea polyacrylamide gel. Fprobe fluorescence was visualized with a Bio Rad ChemiDoc MP imaging system.

Results and Discussion

Synthesis of Processable PANI

The first step in fabrication of a PANI-based sensor of nucleic acids was to generate PANI that was dispersed in water to permit association with probe oligos and targets. To achieve this association, PANI was synthesized by micellar-aided polymer synthesis, as previously reported (Namgoong, Woo, & Lee, 2007). Micelles were generated using a fixed proportion of sodium dodecyl sulphonate (Na-DBS) and ammonium persulfate (APS). The surfactant Na-DBS allows emulsion polymerization of aniline monomers, which facilitates better solubility in a chloroform-water mixture. The polymerization process is a micelle-aided polymer synthesis (Figure 5), and the reaction

occurs at micellar-water interface. The micelle formation is in dynamic equilibrium with the concentration of monomer-surfactant in the reaction solution (Tsotcheva, Tsanov, Terlenmezyan, & Vassilev, 2001; Jia, Kornemandel, Lamhot, Narkis, & Siegemann, 2002).

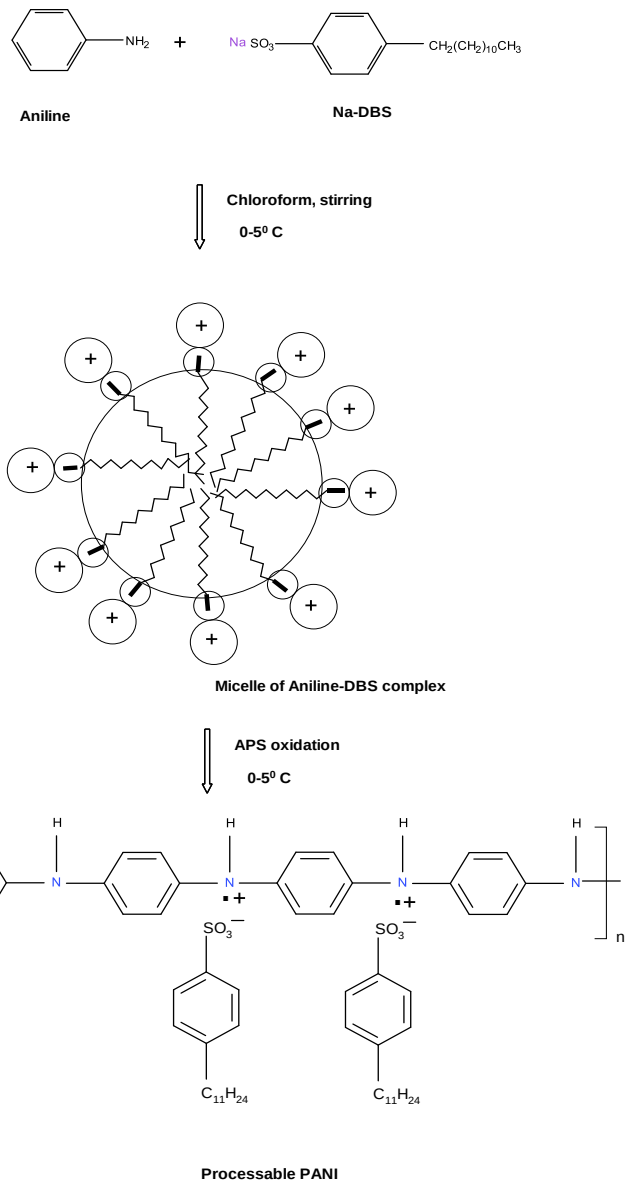

Figure 5. Synthesis of processable PANI

Figure 6 shows the actual pictorial representation of different stages of PANI synthesis.

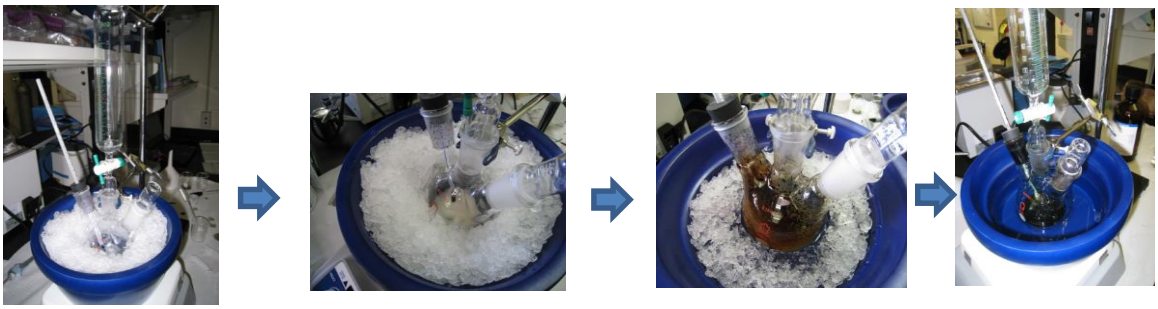

(a) (b) (c) (d)

Figure 6. (a) Start of polymerization reaction (b) after 30 min of adding the APS (c) after 1 h deep brown solution (d) green soluble product after 48 h

Under such conditions, the micelles, formed in the reaction solution, accelerate the polymerization of monomer and allow PANI to develop into a high molecular weight molecule while still dispersed in the oil-water reaction mixture, preventing coagulation and precipitating out of the solution (Kim, Oh, Han, & Im, 2001). The presence of micelles also causes variation in the morphology and size of the PANI molecular structure.

The UV absorption spectrum of synthesized PANI-DBS dispersion (Figure 7) shows a shoulder-like absorption around 350 nm corresponding to π-π^* benzenoid transition, and a strong absorption of a polaron band at 750 nm. The latter is an indication of doped PANI in exciton transition (Yang, Ding, Chen, & Li, 2007; Han, Kusunose, & Sekino, 2009).

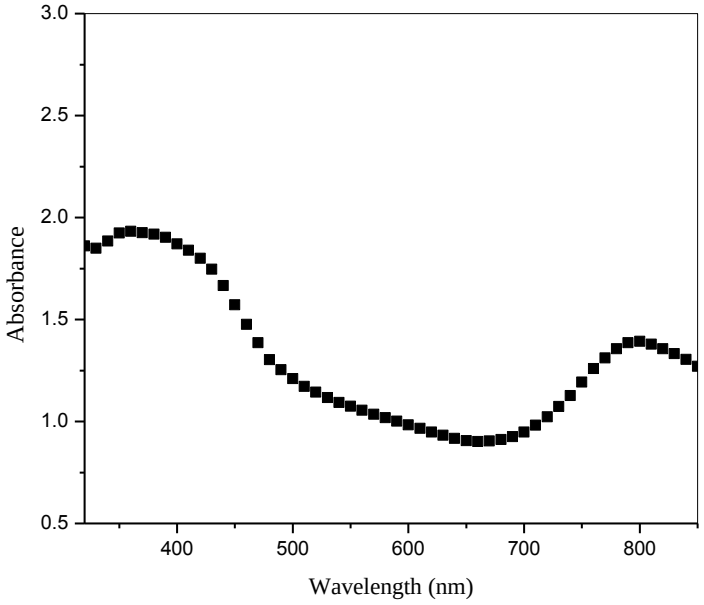

Figure 7. UV spectrum of synthesized PANI-DBS

The product PANI obtained from emulsion polymerization was confirmed by (FT-IR) analysis, which demonstrated a spectral profile as previously described (Figure 8) (Abdolahi, Hamzah, Ibrahim, & Hashim, 2012). The peak at 825 cm^{-1} results from the out-of-plane H deformation of aromatic rings in PANI molecules, whereas the peaks at 1500 and 1600 cm^{-1} are representative of benzenoid and quinoid moiety of PANI. The characteristic peaks of both PANI and the surfactant DBS were observed at 3450 cm^{-1} which corresponds to –NH stretching of PANI, while the peaks at 1060 cm^{-1} and 1010 cm^{-1} are due to S=O stretching and –CH stretching of benzenoid rings present in the DBS molecule, respectively (Table 1).

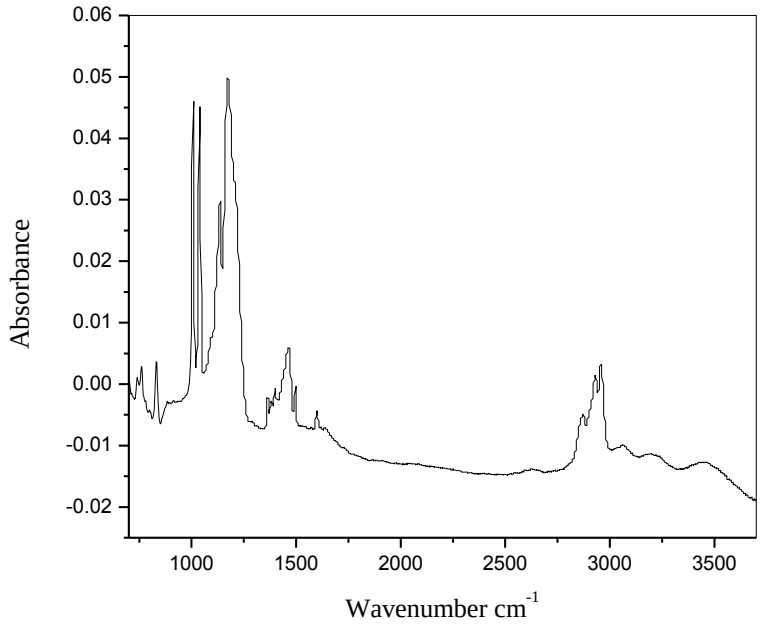

Figure 8. FTIR spectrum of synthesized PANI-DBS

Table 2

FTIR Characteristic Peaks of PANI-DBS

Characteristic bands	Peak position (cm^{-1})
1. Out of plane H deformation of aromatic rings	825
2. C-H stretching of benzenoid rings of DBS	1010
3. S=O stretching	1060
4. C-C stretching	1170
5. Benzenoid stretching	1500

Table 2 (continued).

Characteristic bands	Peak position (cm^{-1})
7. Aliphatic C-H stretching	2950
8. N-H stretching	3450

Electrostatic Bonds between PANI and DNA Probe Oligos Enhanced by UV

In this sensor design, DNA probe oligos were attached to disperse PANI by electrostatic interaction. These oligos were complementary to *let-7*, with the ultimate objective being detection of this micro RNA. However, distinguishing target nucleic acids in a complex biological mixture is a problem for a PANI-based that uses hybridization. As discussed above, PANI spontaneously binds to nucleic acids making detection of electrochemical changes caused by target hybridization indistinguishable from non-specific interaction of DNA or RNA with the CP (Kircheis, Blessing, Brunner, Wightman, & Wagner, 2001; Wolfert et al., 1999). To address this, UV irradiation was used to bond probe oligos to PANI. Exposure of polymer surfaces to UV can create polar species and localized charge units increasing wettability (Kadashchuk et al., 2007). UV treatment of PANI and probe DNA solution should make the π-π* bond in PANI, which is more labile and potentially enhances electrostatic bonds that could form with the negative phosphate groups of probe DNA oligos. The increased bonding will improve differentiation of probes attached to PANI versus spurious association of nucleic acid from a biological sample.

The optimal UV exposure time of PANI-DBS and ssDNA mixture was determined by irradiating at an intensity of 100 μJ/cm^2 for various time intervals. Both the steady state emission and excitation maximum fluorescence intensity show a similar trend as the time of UV exposure of the PANI-DNA complex was adjusted (Figure 9 and Figure 10).

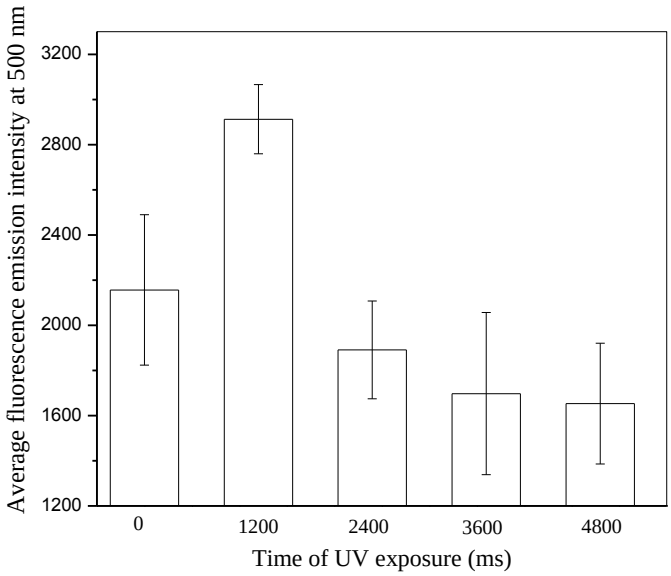

Figure 9. Optimization of UV exposure by fluorescence emission intensity of PANI-DNA probe complexes

The higher emission fluorescence intensity at 1200 ms of UV exposure possibly shows electron flux in PANI from phosphate groups of DNA probes (Figure 9 and Figure 10). This suggests a high electrochemical adsorption of the negatively-charged DNA on positively-charged PANI. The increased excitation and emission at 1200 ms indicate that the electron flux from phosphate groups to the delocalized PANI structure increases the benzenoid-conjugated state of PANI, resulting in higher excitation energy at 350 nm (Rahman, Li, Lopa, Ahn and Lee, 2015) (Figure 9 and Figure 10). At longer exposure times, the fluorescence emission intensity decreases which could potentially be the result

of covalent bond formation between quinoid moiety of PANI and nitrogenous bases of DNA (Blount & Tor, 2003).

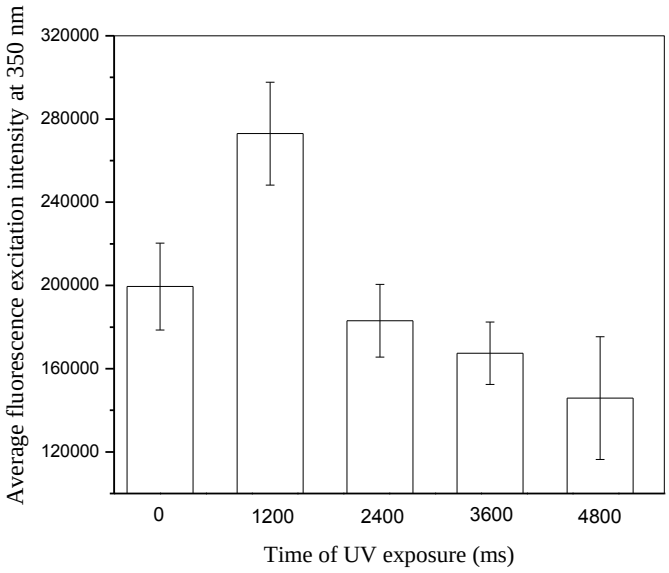

Figure 10. Optimization of UV exposure by fluorescence excitation intensity of PANI-DNA probe complexes

Determining the optimal amount of PANI and probe, comprising a sensor, is important for establishing a platform suitable for analysis of biological samples. To assess this, different concentrations of probe oligos were tested for their ability to induce changes in PANI fluorescence (Figure 11). Two concentrations of PANI were tested, and both showed that as the concentration of probe was decreased, there was a concomitant reduction in fluorescence. The threshold for detection of associated oligos was an effect of the mass ratio of PANI to oligo. At the highest concentration of PANI (~2400 µg), the lowest amount of oligo that affects fluorescence of the CP was 1 ng. When the lower amount of PANI (~240 µg) was used, the lower limit of probe was 0.1 ng. At higher concentrations of probe, the average fluorescence intensity of PANI-probe adduct decreases below base fluorescence intensity. This could be due to covalent bonding

between imine groups of PANI and DNA nitrogenous bases resulting a loss of fluorescence (Blount & Tor, 2003; Wanekaya, Chen, Myung, & Mulchandani, 2006).

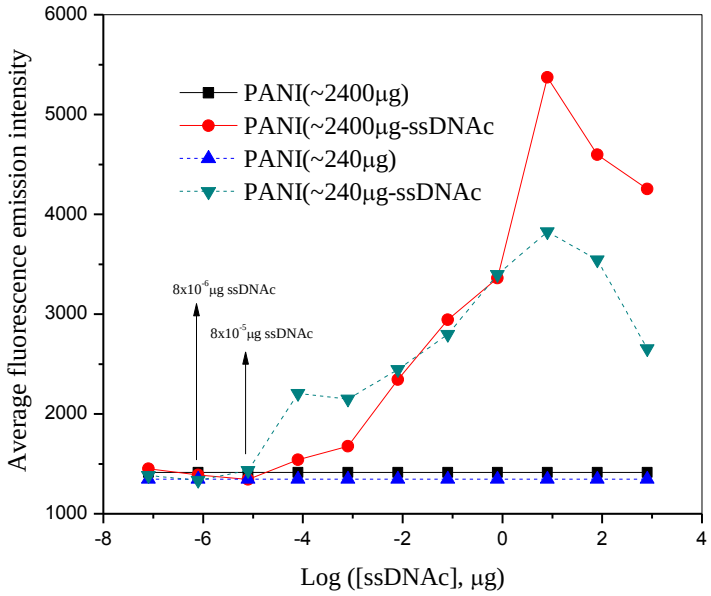

Figure 11. Sensitivity study pf PANI-DNA probe complex

Immobilization of PANI with Phosphate Groups of Probe Oigos

FTIR was used to characterize the immobilized PANI with the phosphate groups of the DNA probes. The FTIR spectra shows higher electrostatic bonding of PANI-probe complex by UV exposure (Figure 12). A stronger phosphate-PANI bond at 1270 cm^{-1} was observed when PANI-DNA was subjected to UV irradiation for 1200 ms. The sugar phosphodiester bond and the N-H stretching of purine and pyrimidine bases were observed at 800 cm^{-1} and 1575 cm^{-1}, respectively. This shows probes are electrochemically adsorbed in the PANI structure through electrostatic bonding between the negatively-charged phosphate groups of DNA and positively charged doped PANI.

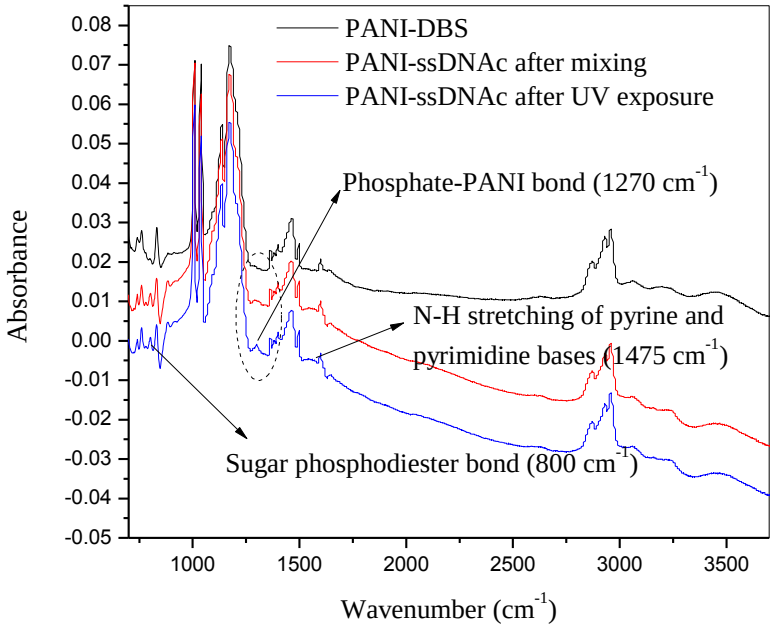

Figure 12. FTIR spectra of PANI, PANI mixed with DNA probe, and after UV exposure of PANI-DNA probe mixture at 100 μJ/cm^2 for 1200 ms

Thus, electrostatic bonds between probe phosphate and PANI amine groups are the interaction strengthened by UV exposure (Figure 13). Importantly, probes associated with this method should be free to base pair with DNA/RNA since we do not observe interaction of PANI and probe nitrogenous bases (Figure 3B). The optimized UV treatment established here provides enhanced association of probes without the formation of covalent bonds between probe bases and PANI (Ahuja et al., 2007; Cosnier, 1999).

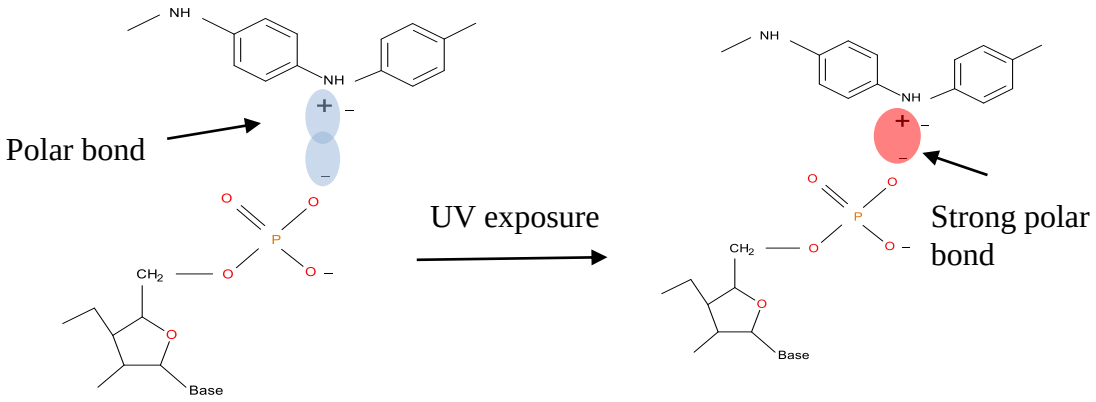

Figure 13. Mild UV exposure enhances the interaction between the phosphate groups in ssDNA and PANI. Stronger electrostatic bond by UV irradiation of PANI-DNA probe adduct.

Next, the nanostructure of PANI particles was determined before and after association with DNA oligos. Light scattering was used to assess the size of PANI particles present in the chloroform/water emulsion (Figure 14). A heterogeneous range of particles was observed that spanned approximately 1000nm to 100nm. Association of DNA oligos had a negligible effect on the overall particle population though there was minor skewing to slightly smaller sizes. This may reflect the dynamic nature of the emulsion in which the particles are suspended, or effects of exposing PANI to UV. The morphology of PANI was also inspected as a film before (Figure 3B) and after (Figure 15) DNA immobilization by SEM. Attachment of DNA caused the film to develop a more heterogeneous structure, which, like the effect on particle size, may be the result of UV irradiation. To verify the association of DNA with PANI, EDS was performed to identify elements associated with PANI (Figure 16). After immobilization of DNA probes with UV, PANI films were extensively washed with SDS, and despite the use of

this harsh treatment, phosphorous was observed indicating that probe oligos were attached.

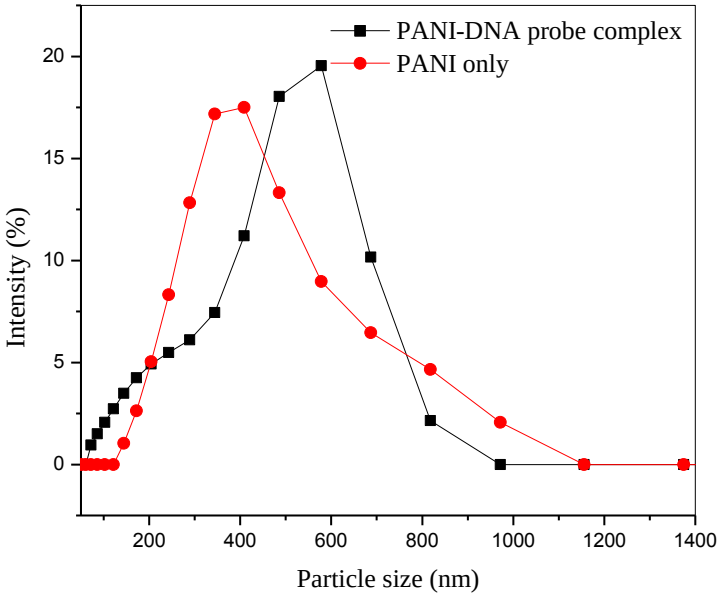

Figure 14. Particle size of PANI and PANI-DNA probe complex

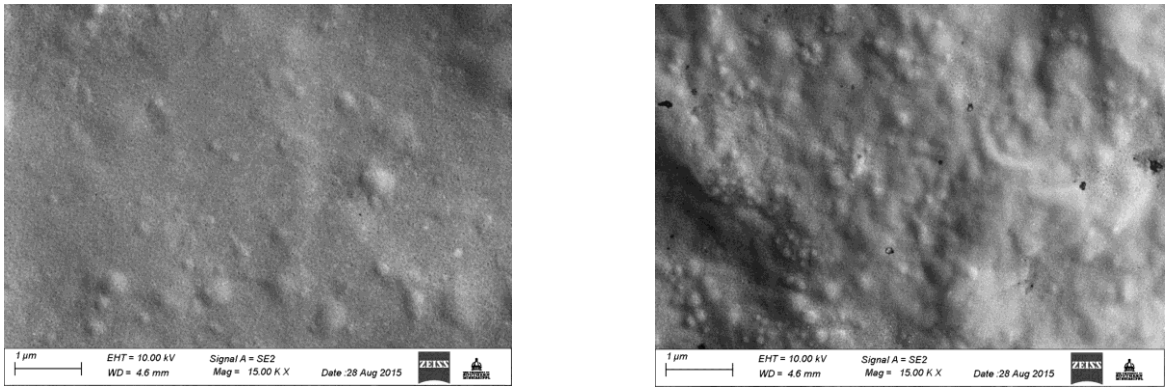

(A) (B)

Figure 15. SEM images of (A) PANI and (B) PANI-DNA probe complex

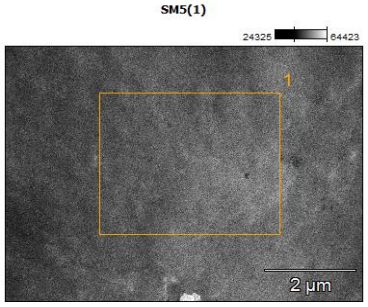

Image Name:	SM5(1)
Image Resolution:	512 by 384
Image Pixel Size:	0.02 µm
Acc. Voltage:	20.0 kV
Magnification:	15000

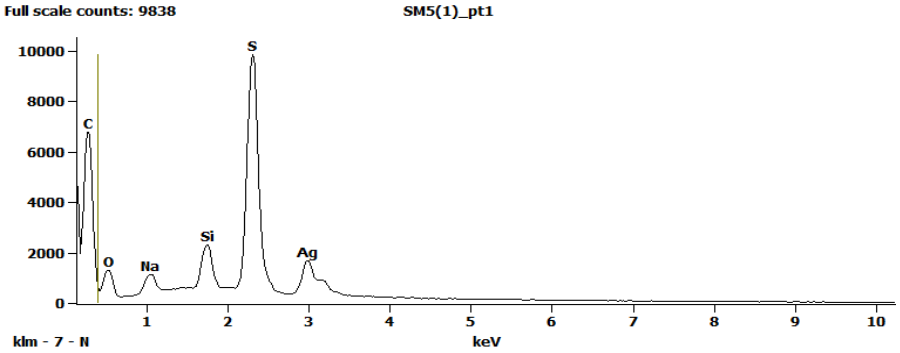

(A)

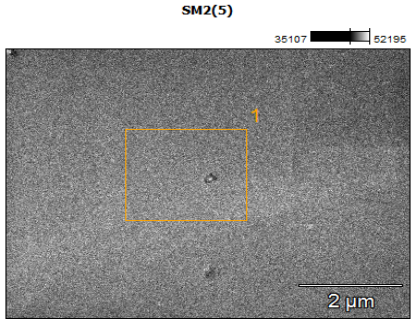

Image Name:	SM2(5)
Image Resolution:	512 by 384
Image Pixel Size:	0.02 µm
Acc. Voltage:	20.0 kV
Magnification:	15000

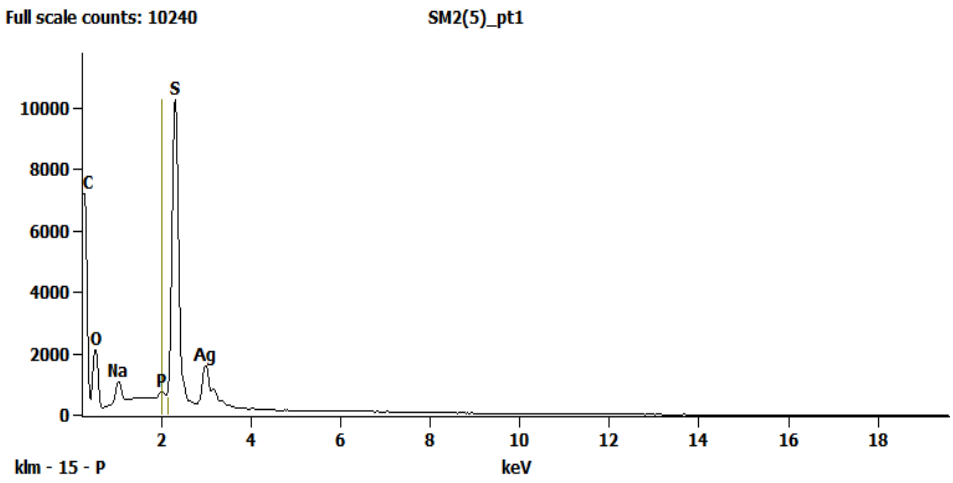

(B)

Figure 16. EDS images of (A) PANI and (B) PANI-DNA probe complex

Detection of Hybridization

It was previously reported that hybridization caused non-covalently bonded probes to dissociate from PANI and other varieties of CPs (Zhang et al., 2011b). The proposed mechanism was that the nitrogenous bases of probes mediated bonding with CPs, and after hybridization to a complementary nucleic acid, they were no longer available to attach. If this were the case, the expectation would be reversion of PANI properties to their state before attachment of probes. To test if UV-enhanced bonded probes behave in the same way, hybridization was performed with complementary DNA oligos. Initially, UV spectroscopy was used to determine the polaron (880nm)/benzenoid (350nm) ratio of PANI before and after hybridization (Figure 17). The benzenoid band of the π conjugated conducting polymers is representative of the electron density of the molecule in a labile state, while the polaron band represents the doped state of the polymer (Kar, 2013). The higher electron flux from phosphate groups of attached probes results in lower localization of excited species like excitons leading to lower doped states

(Salaneck, Friend, & Bredas, 1999). After hybridization of complementary oligos, PANI regained its higher doped state.

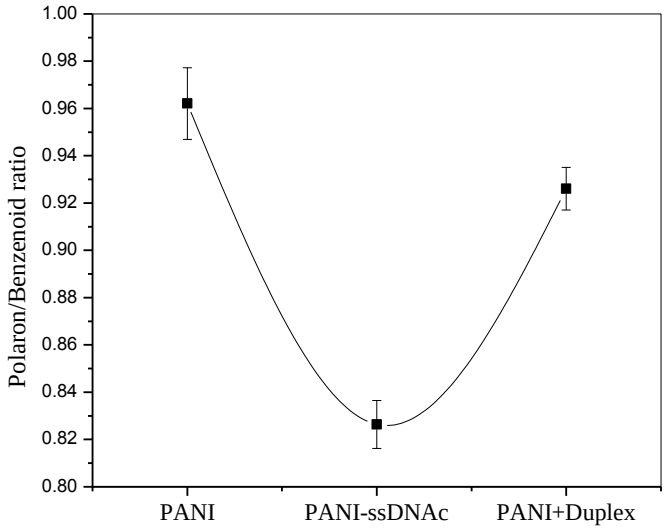

Figure 17. Polaron/benzenoid ratio of PANI, PANI with attached probe (PANI+probe) after hybridization with a complementary oligo (PANI+probe+comp)

Next, changes in the intensity of PANI fluorescence emission was investigated before and after hybridization. Similar to what was observed with UV spectroscopy, hybridization of complementary oligos reduced PANI fluorescence, caused by association of probes (Figure 18). This effect was highly specific to the sequence of target oligo, added during hybridization. Introduction of a single mis-match into the oligo significantly impaired restoration of PANI base-fluorescence when hybridization was performed with a complementary oligo. Similar to other CP platforms that use

electrostatic attachment of probes, this indicates that a PANI-based sensor with UV-immobilized probes will be highly specific to target nucleic acids.

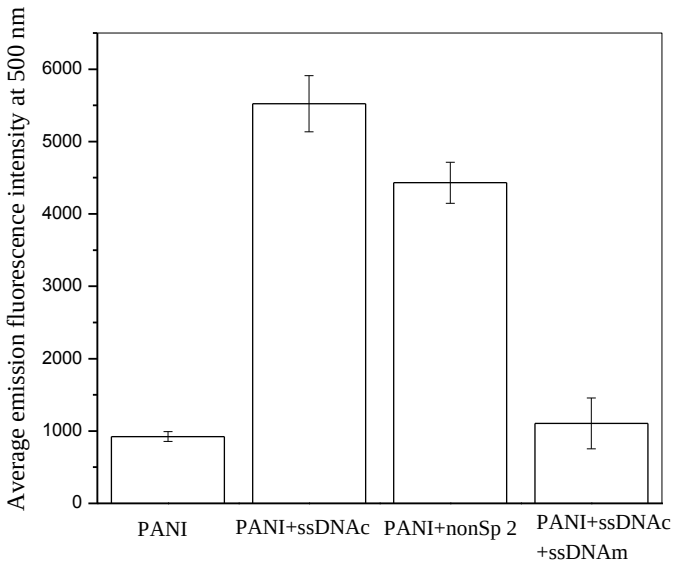

Figure 18. Changes in PANI fluorescence at 500 nm before and after hybridization, measurements were made before probe attachment (PANI), after probe attachment (PANI+probe), after hybridization with oligos with one mis-match (PANI+probe+1 mis oligo), or hybridization with a 100% complementary oligo (PANI+probe+comp)

Next, PANI coated on borosilicate glass was tested as a format for the sensor platform (Figure 19). Fluorescence of the PANI film was observed using conventional fluorescent microscopy. After coating, probes were electrostatically adsorbed to PANI and irradiated by UV, which is seen in dispersed PANI having increased fluorescence. Hybridization was then carried out with complementary oligos. Similar to what was observed with PANI dispersed in water, a dramatic loss of fluorescence was observed upon hybridization. Together, these results demonstrate that PANI can be utilized to detect nucleic hybridization without the need for secondary detection or covalent probe attachment.

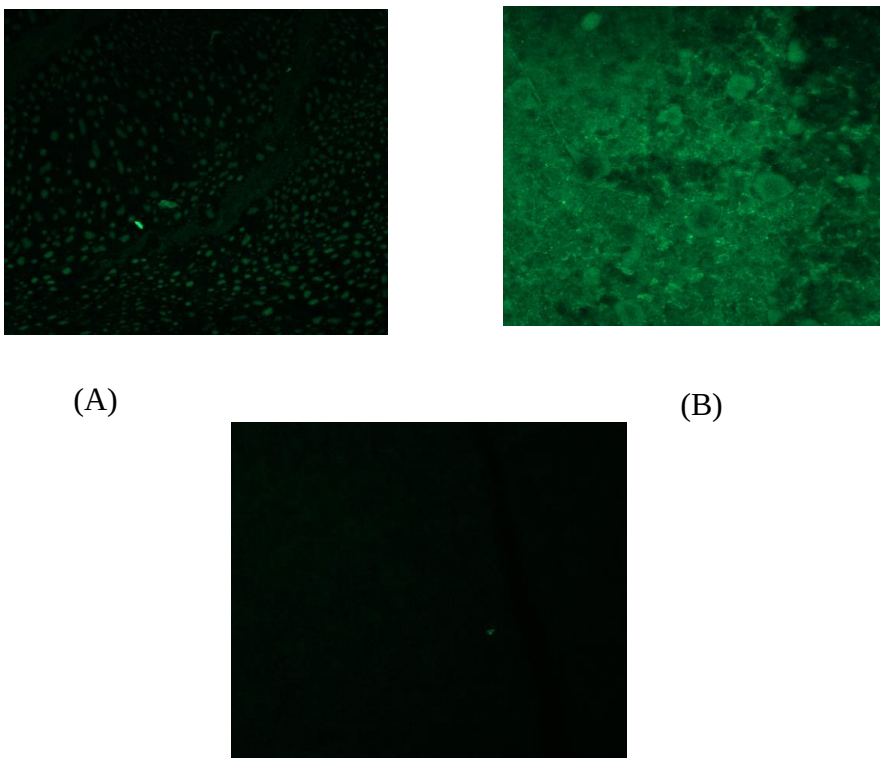

Figure 19. Fluorescence microscopy showing images of (A) PANI coated on plastic (B) coated PANI-ssDNAc (C) coated PANI-ssDNAc + ssDNAm

Hybridization Causes Dissociation of Probes from PANI

The results of hybridization experiments with UV immobilized probes were consistent with the previously described dissociation from CPs after hybridization (Zhang et al., 2011b). To confirm dissociation, the presence of a dissociated probe was monitored in hybridization solution (Figure 20A). A probe labeled with 6-fluorescein amidite (6-FAM) was attached to PANI by UV, and subjected to hybridization. After pelleting of PANI by centrifugation, the supernatant was separated by electrophoresis on an 8M urea denaturing polyacrylamide gel (Figure 20A). In the absence of target oligo, very little Fprobe was found in the supernatant. However, when complementary oligo was added, a large amount of Fprobe was observed in the supernatant indicative of probe dissociation.

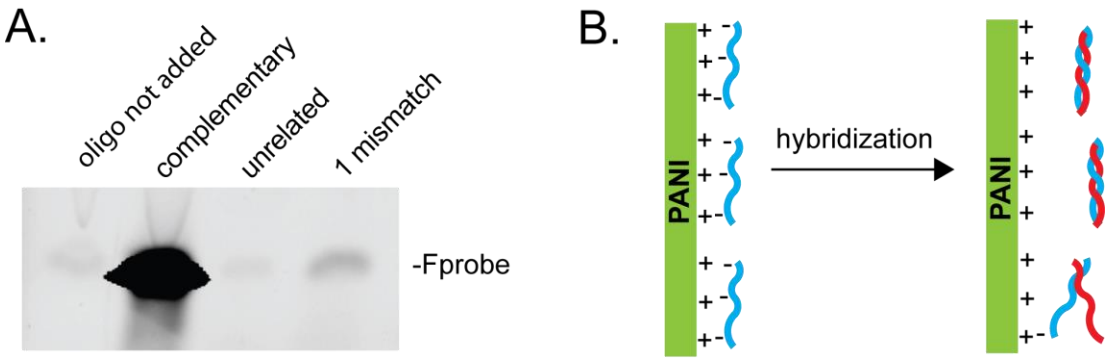

Figure 20. Hybridization of immobilized probes results in detachment from PANI. (A) Imaging of FAM conjugated let-7 oligo probe (Fprobe) after urea-PAGE electrophoresis. Fprobe was immobilized on PANI and mixed with hybridization buffer (PBS). After a fifteen-minute incubation, PANI was removed by centrifugation, and the supernatant was loaded on a urea-PAGE gel. In lane one, no oligo was added. In lane two, a DNA oligo complementary to Fprobe was added. In lane three, an oligo of unrelated sequence was added. In lane four, an oligo was added that was had a single mismatch to the Fprobe. (B) Diagram shows detachment of probes from PANI after duplex formation with complementary target nucleic acid.

In contrast, minimal probe dissociation was observed when hybridization was carried out with oligos with an unrelated sequence, or oligos containing a single mis-match. Similar to the non-hybridized condition, the addition of unrelated oligo did not result in any appreciable increase in dissociation of Fprobe. Hybridization with the single mis-match oligo did result in some dissociation of probe, but was dramatically less than when using perfectly complementary oligos. These results reconfirm that detachment of UV immobilized probes occurs after hybridization (Figure 20B). Based on these results, the electrostatic interaction between phosphate groups of DNA and PANI is a major driver of association. Thus, it would appear that the formation of the helical structure of double-stranded DNA might lead to conformational changes–breaking the electrostatic interaction. Furthermore, the ability of a single mismatch to inhibit dissociation highlights the stringency for formation of perfectly helical DNA devoid of bulges due to unpaired bases.

Sensitivity and Specificity of PANI Sensor

Finally, experiments were performed to assess the sensitivity and specificity of the PANI-based sensor. The detection range was determined by hybridizing a series of complementary oligo concentrations to PANI-probe complexes (Figure 21). The fluorescence intensity of PANI was then measured to evaluate the ability of the different amounts of complementary oligo to restore base PANI fluorescence. When complementary oligo was added in molar excess of attached probes, higher fluorescence was observed due to direct interaction of oligo with PANI. Equimolar amounts of complement completely restored PANI fluorescence. At other concentrations, there was a clear trend showing decreasing the amount of complement resulted in less reversion of PANI fluorescence. Ultimately, the sensor is able to detect a complementary oligo that is present at a concentration around 10 pM. Optimization of PANI and probe concentrations will likely yield even greater sensitivity. Cogent to this point, multiple concentrations of PANI and probe could be used to construct a viable sensor. Determining the most efficacious amount of PANI and probes in a biological sensor will be the focus of future work. However, despite the non-optimized nature of the sensor system presented here, the detection limit was lower than other probe-dissociation-based sensors or those that don’t use secondary detection (Rahman, Li, Lopa, Ahn, & Lee, 2015; Kar, 2013).

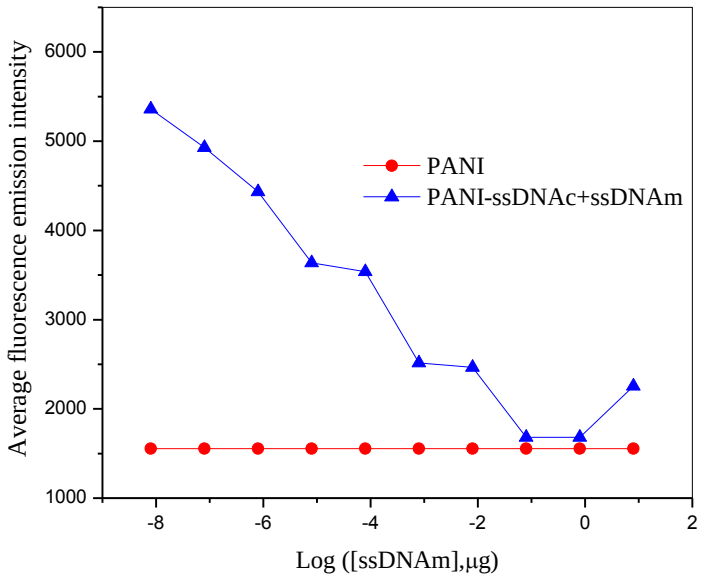

Figure 21. PANI fluorescence after hybridizing increasing concentrations of complementary oligo

The performance of the sensor was tested with a biological sample by detecting a specific transcript in total RNA extracted from *Drosophila melanogaster* (fruit flies). Throughout this study, the probes attached to PANI were designed to be complementary to the micro RNA *let-7*. This micro RNA is not consistently expressed across the stages of the fruit fly life cycle. It is present in adult flies, but not in early stages such as larva. Total RNA was extracted from adult and larval flies. Total RNA (1 µg) from each sample was hybridized to PANI-probe complexes (Figure 22). Consistent with the expression of *let-7* in adult flies, after hybridization, a strong reduction of PANI fluorescence was observed. This reduction was not seen when hybridizing PANI-probes with RNA extracted from larva, which do not express *let-7*. This result indicates that the platform is sufficiently robust to detect the presence of a specific nucleic acid even when confronted with the complex mixture of nucleic acids comprising biological samples.

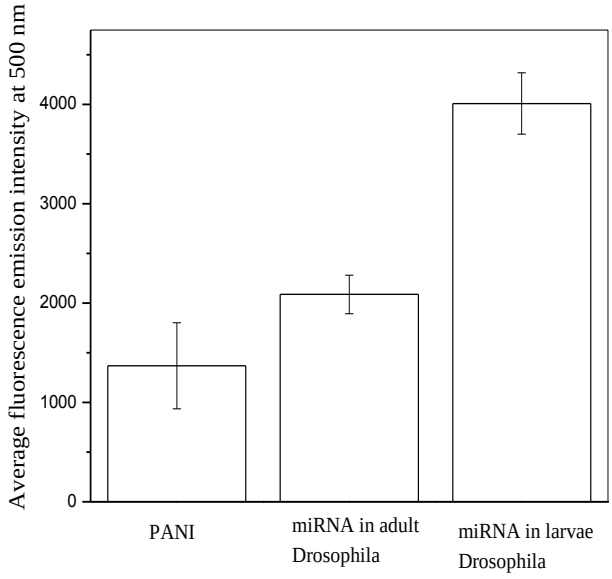

Figure 22. Detection of *let-7* miRNA in total RNA isolated from adult (let-7 expressing), but not in larval (no *let-7* expressed) fruit flies

Conclusions

In this research, a sensor of nucleic acids was developed based on PANI and UV-immobilized probes. PANI was synthesized by micelle-aided polymerization with sodium dodecyl benzene sulfonate, resulting in water dispersible PANI that was able to interact with nucleic acids in solution. A strategy was developed for electrostatic immobilization of probes oligos on PANI that used enhancement by UV irradiation. Increased binding of PANI to probes from UV exposure significantly altered the fluorescence of PANI. This expsoure allowed for the attachment of probes without the formation of covalent bonds, while utilizing properties of PANI in signal detection. Furthermore, this platform was capable of detecting hybridization of oligos complimentary to probes with great specificity, distinguishing between perfectly complementary oligos and ones only having a single mismatch. The platform also demonstrated high sensitivity and was capable of

detecting amounts of target oligo lower than other published methods that used probe-dissociation based transduction or detection without secondary compounds (Sabirmeeza & Subhashini, 2013; Yang et al., 2007). The sensor was also robust enough to detect expression of a small RNA in total RNA extract. Finally, we show that the sensor relies on dissociation of probes via duplex formation to transduce hybridization. This configuration of the sensor provides several improvements on previous strategies. A label is not used, and this reduces the overall cost of fabrication, minimizes the complexity of the analysis, and excludes the need for fluorescent probes, which might affect the binding interactions (Kerppola, 2008). Finally, other reports describing sensors based on probe dissociation rely on fluorescent labels, and could not take advantage of all CP properties to transduce hybridization. Future work will be aimed at exploiting other properties of PANI, such as electrochemical methods, to detect nucleic acids.

CHAPTER III

POLYANILINE COATING ON BOROSILICATE GLASS AS A 2D FLUORESCENT SENSING PLATFORM FOR DETECTION OF DNA MIMIC TO MICRO RNA *LET-7*

Introduction

The surface of water dispersible CPs' coating undulations can cause clustering artifacts when the distribution of immobilized and hybridized adducts is recorded in a two-dimensional projection. Therefore, for a uniform coating, there is a need for an artificially weather-coated surface, say borosilicate glass, through simultaneous ultraviolet (UV) and moisture exposure. Water drastically changes the physical properties of glass, including increasing thermal expansion and specific volume and decreasing viscosity (DeRosa, Schader, & Shelby, 2003). Simultaneous UV and moisture treatment increases glass density, refractive index, and decreases the surface tension (Efimenko, Wallace, & Genzer, 2002). This can result in a uniform coating of water dispersible CP on glass surface caused by hydration of glass which is diffusion of molecular water into glass by UV/H_2O treatment (Sharma, Modi, & Bansal, 2015). The contact angle of borosilicate glass is usually high, and this results in separation and sagging of the coating layer of water dispersible CPs on drying on untreated glass (Bowman, 1998). However, the UV/H_2O treatment reduces the contact angle and results more uniform coating layer (Yu, Chong, Tor, Liu, & Loh, 2015). UV light causes breakdown of glass at molecular level (Khrapko, Lai, Casey, Wood, & Borrelli, 2014). The cutoff wavelength of UV is 170 nm for fused silica and 310 nm for borosilicate glass (Escoubas, Gatto, Albrand, Roche, & Commandre, 1998). The free glass surface contains free silanol groups and superficial hydrogen-bonded silanols. Hydration leads to water physisorbed on irradiated

glass surface and creation of hydrophilic surface. (Chen, Li, Zhao, & Zheng, 2010) To increase the uniformity of the coating on treated glass and make CPs more hydrophilic, we attempt *in-situ* blending with other hydrophilic and water-soluble polymers. Different polymers, like polyethylene glycol (PEG) and polyvinyl alcohol (PVA), have been used to prepare hydrophilic CP composites (Zhu & Marchant, 2012). Micro to nano composites of PANI have attracted even more interest because of their properties which make them suitable for chemical sensors, batteries, light-emitting, and electronic devices (Pethe & Kondawar, 2014; Shi et al., 2015). The PEG/PVA was dissolved in distilled water with stirring, and then the viscous solution was transferred in the reaction pot of in situ polymerization of CP monomer in presence of oxidant and polyelectrolyte for water dispersibility. The auxiliary polymer PEG/PVA improves the viscosity and wettability of the CPs on the itched glass surface. For generation of cluster maps, a pseudo-colored cluster heat map was interpolated at high resolution by MATLAB (Owen, Williamson, Magenau, Rossy, & Gaus, 2012). The green color fluorescent is extracted from the surrounding black by color thresholding, and each pixel values are stored in a matrix variable. The other colors, except green, are filtered out, and the green is further dilated several times by morph function. The intensity of single value points was determined by region properties and from their histogram intensity distribution the fluorescence intensity is calculated. In this research work we attempt to develop a 2D fluorescent sensor using PANI-PEG blend for uniform coating on borosilicate glass and using MATLAB software to determine the pixel intensity of the fluorescent signature of immobilization of DNA probe and hybridization with the target nucleotide.

Experimental

Materials

Aniline and ammonium peroxydisulfate were purchased from Fisher Scientific, USA. Sodium dodecylbenzene sulfonate (Na-DBS) was purchased form Pfaltz & Bauer, USA. Chloroform was obtained from EMD Chemicals, USA. Polyethylene glycol (PEG 800) was purchased from Fisher Scientific. Borosilicate microscope cover glass was also obtained from Fisher Scientific. All the reagents were analytical grade, and they were used without purification. Water used in all measurement and solutions was DNase/RNase free distilled water.

PANI-PEG Blend Synthesis

Aniline (1 mL, 11 mmol) was completely dissolved in 60 ml of chloroform in a 250 mL round bottom flask, and the solution was stirred at 600 rpm and cooled to 0 °C. Na-DBS (7.44g, 21 mmol) was added into the aniline solution and stirred vigorously at 0-5 °C. APS (3.072 g, 13.5 mmol,) was dissolved in 20 mL water in a beaker along with 0.25 g (0.03 mmol) and added drop wise into the reaction mixture for 120 min to avoid overheating of the reaction mixture. The reaction mixture was stirred at 0-5 °C for 24 h, and allowed to reach room temperature for 24 h. The reaction mixture initially turned to milky white, then dark brown, and finally into a dark green colored PANI-DBS dispersion in chloroform-water mixture. The resultant PANI-DBS solution was filtered in a Buchner funnel and then mixed with 80 mL chloroform and 120 mL water in a separation funnel. The solution stood for 24 h after which the dark green PANI was collected from the separation funnel, while unreacted DBS and APS were left in the aqueous supernatant.

Treatment of Borosilicate Glass Substrate

Measurement of contact angle of treated borosilicate glass with PANI-PEG blend Borosilicate cover glass was done after washing with acetone and centrifuged with isopropyl alcohol for 5 min. Then it is oven-dried for 1 h. The glass was dipped in 50 µl of water in a petridish such that the water surface barely immerses the borosilicate glass surface. The glass immersed in water was irradiated at 100 $\mu J/cm^2$ of UV irradiation for 10 min. The borosilicate cover glass was then dried and kept in oven for 2 h.

SEM image analysis of coating surface

The PANI-PEG solution was coated on a silicon wafer by drop coating. High-resolution field emission SEM (FE-SEM) was imaged with Zeiss Sigma Variable Pressure, Field Emission Gun Scanning Electron Microscope at 10 kV in high vacuum mode with a Thermo energy dispersive and wavelength dispersive X-ray detectors (EDS/WDS) at an accelerating voltage of 20 kV. Samples were sputter coated with silver at instrument reported thickness of 5 nm. Two different magnifications were used for imaging one at 3000X and other at 18000X.

Measurement of Fluorescence Spectra

A camera from Leica IMC S80 at 20X magnification captured the fluorescence image of the borosilicate glass coated PANI-PEG. The grayscale image was processed green by LHS 44.5 software Exposure, Gain and Gamma were kept fixed at 735 ms, 2.9X and 5.5, respectively.

Color Thresolding with MATLAB

The fluorescence image was stored in .tif file, and MATLAB code was created to determine the threshold value of the color image. The threshold value helps in creating

the foreground image representing the fluorescent active region. The pixel value of the foreground image was determined at several spots, and the average was taken for a representative pixel value of the fluorescent active region.

Results and Discussion

Synthesis of PANI-PEG Blend

The PEG mixed with APS in 20 ml water was added very slowly for 2 h to form a coherent blending of the PEG with the in situ formation of PANI. Figure 23 shows SEM image of the same spot at two different magnifications of 3000X and 18000X. We can see a loose binding of the PEG on the background PANI structure. A perfect encapsulation was not achieved, although such 100% encapsulation would markedly reduce the property of PANI, which we did not intend. However, a loose binding does serve the purpose of increasing the hydrophilicity of PANI, which would result a uniform coating on treated borosilicate glass surface.

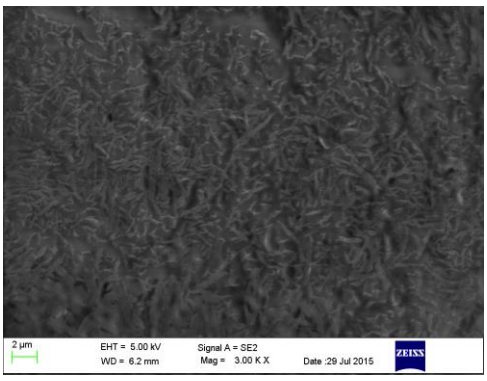

(A)

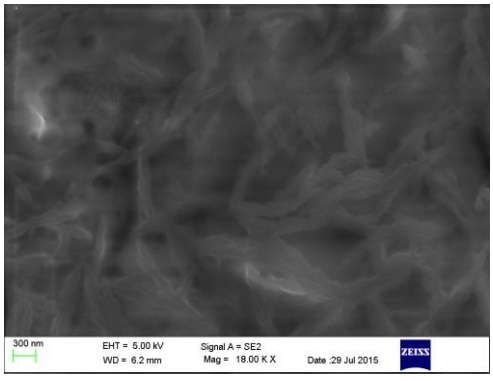

(B)

Figure 23. Coating of PANI-PEG blend on treated borosilicate glass (A) magnification 3K X (B) magnification 18K X

Treatment of Borosilicate Glass and Measurement of Contact Angle

Borosilicate glass surface was chosen because it is very flat and conducive to uniform coating; however, the surface energy was also very high and needed to be tuned for uniform coating with PANI. Figure 24 shows that both UV and water have profound effect on glass surface (Faure et al., 2013). The UV-water combination reduces contact angle of glass surface from high as 70 to low as 20. The radical transformation to hydrophilicity of borosilicate glass surface depends on time of exposure and results in removal of free silanol groups and deposition of a surface water layer or formation of gel layer.

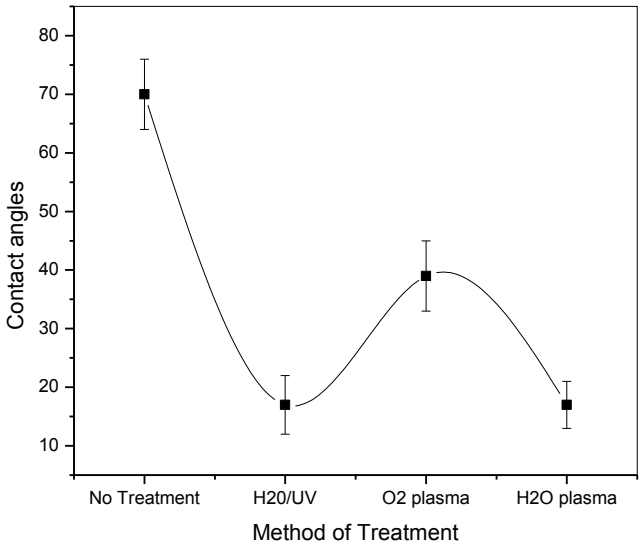

Figure 24. Contact angle of various treatments of borosilicate glass

Coating of PANI-PEG Blend on Treated Borosilicate Glass

The PANI coated on borosilicate glass surface shows visible undulations, which would impair fluorescence measurement. There was visible separation of coating from glass surface showing surface energy of glass surface, to be much higher than

chloroform-water-dispersed PANI. There was some improvement on reduction of contact angle of borosilicate glass by UV-H_2O treatment, but still, there was more scope of fine-tuning for uniform coating. The in-situ blending of PANI with PEG resulted in uniform coating, causing further reduction of surface energy of PANI by loosely coupled hydrophilic PEG on its surface. Figure 25 shows a significant change of coating texture after UV/H_2O treatment and coating with PANI-PEG blend.

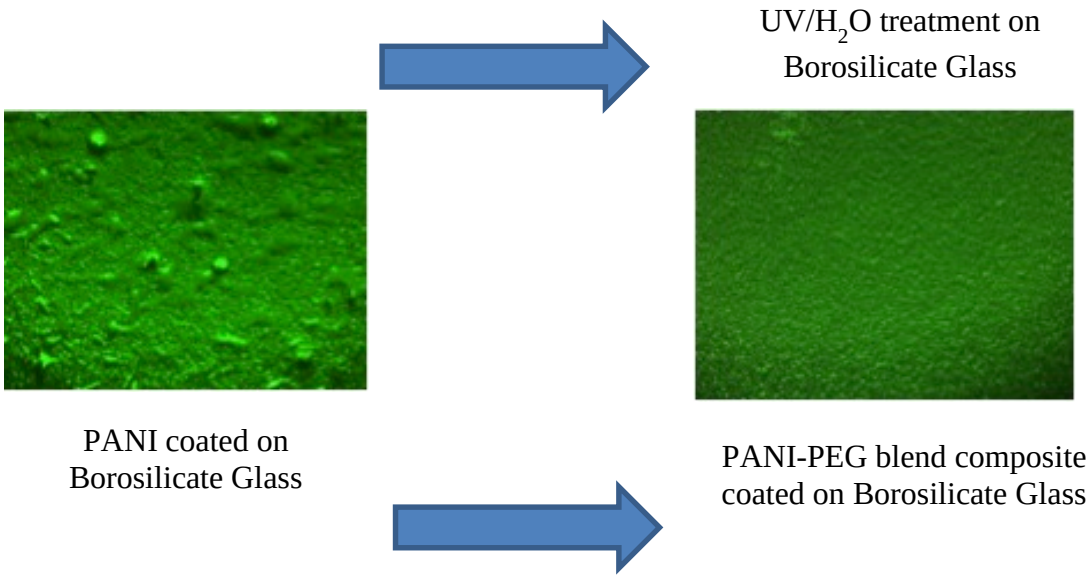

Figure 25. Coating of PANI-PEG blend on treated borosilicate glass

Fluorescence Measurement

Fluorescence of PANI-PEG coated borosilcate glass surface and PANI-ssDNA probe complex and PANI duplex after hybridization are shown in Figure 26. Under same specification of image capture, it was found, according to our previous finding, the immobilization of ssDNA on PANI-PEG surface increases its fluorescence intensity, while hybridization causes detachment of duplex moiety, resulting in decreased fluorescence. The PEG was found to be non-interfering to fluorescence intensity at 500 nm.

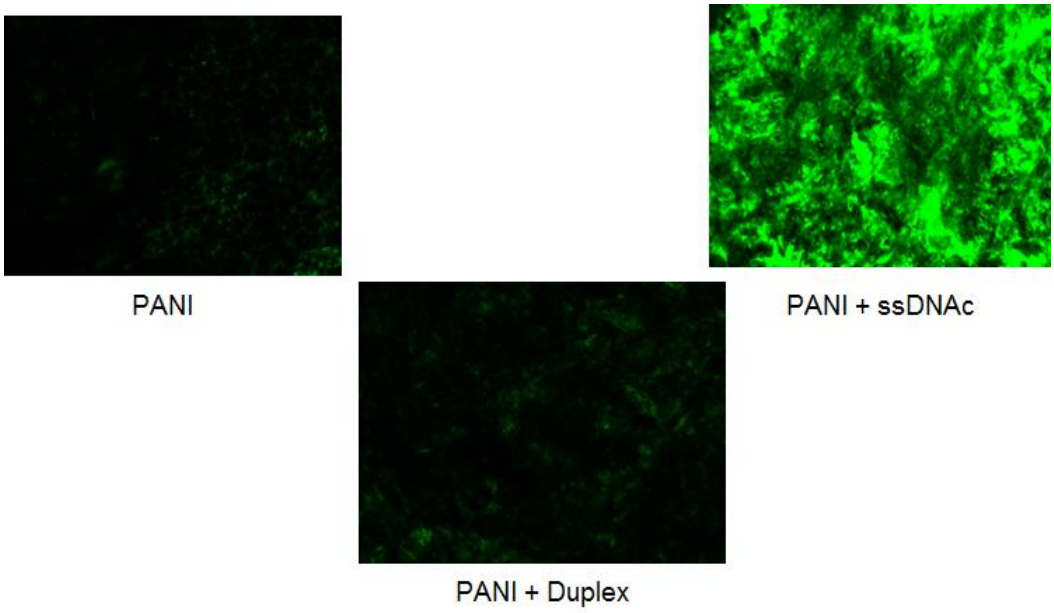

Figure 26. Fluorescent image of the coating of PANI-DNA probe and after hybridization

Image Analysis Using MATLAB

Thresholding is a way to segment images by labeling pixels as belonging to one or more classes, segmented based on intensity (Kahndekar & Samani, 2014). The image is converted to histogram with two or more separate modes, and we can find the threshold that would classify all the pixels greater than the threshold as group 1 and all the pixels less than threshold as group 2. Algorithm 1 is an example of Global thresholding algorithm, which uses an iterative method. An initial guess t for the threshold has been selected and the image has been segmented using the threshold into groups with one having pixel intensity greater that t and other having pixel intensity less than or equal to t. The average for the two groups is calculated and a new threshold, is set with a value midway between the averages. Steps 2 through 4 have been repeated until there is no change. An advantage of this algorithm is that we can use histogram to do all computation because the mean can be easily found by using the probability distribution.

1. Select an initial guess of Threshold t
2. Segment the image using t
    a. Group1 is all pixel having intensities >t
    b. Group 2 is all pixel having intensities <= t
3. Compute average A1 for all pixels of Group 1
4. Compute average A2 for all pixels of Group 2
5. Let t = (A1 + A2)/2
6. Repeat steps 2-5 until no change is observed

Algorithm 1. Heuristic Algorithm for Global Thresholding

There are different methods of segmentation of image, such as fixed circle segmentation, which assign a constant size and shape to all the spots. The diameter of the circle is taken as constant for all spots in the image. This method causes some regions with high intensity areas to be excluded, and some regions with low intensity are included. This is because of the fixed diameter of all the drawn circles despite the variation in the diameter of the spots in the same image. Another method is adaptive circle segmentation that considers the shape of each spot as a circle, where the center and diameter of the circle are estimated for each spot. Although it achieves better result, the adaptive circle segmentation takes shapes including ellipses. Thresholding segmentation gives far better result with global thresholding, has a special advantage.

```
clear all, close all

I = imread ('PANI-Fluo.tif');
[H,W] = size(I);
figure, imshow(I);

% Get histogram. hist(i) is the count of pixels with value x(i)

[hist, x] = imhist(I);
figure, imhist (I);

% Convert to probability
p = hist / (H*W);
t= 128; % initial guess for threshold

while true
disp (t);

% Group 1 is all pixels with intensity > t

m1 = (x>t); % create a logical mask, true when x>t

% Compute mean of group 1

u1 = sum(x(m1). *p(m1)/sum(p(m1));

% Group 2 is all pixels with intensity <= t

m2 = (x<=t); % create a logical mask; true where
x<=t

% Compute mean of group 2
u2 = Sum (x(m2) * p(m2)/sum(p(m2));

tnew  = (u1 + u2) / 2;
if t = tnew

break;  % Quit if no further changes

else
t= tnew; % otherwise this is new threshold
end

end
```

Code 1. MATLAB program for global thresholding

Code 1 is a program that is based on Global thresholding. The PANI-Fluo.tif is read by the function imread. The histogram of the image is obtained by function imhist, and the histogram is converted to probability function by dividing the number of pixels. We start with an initial guess for the threshold. There is an iterative loop with m1(x>t) which is an expression in MATLAB that creates a logical mask of all the intensity values that are greater than T. So it has 1 for those and 0 for the other. The mask is used to compute the value of x and probability p such that the mask is true. Finally, the value of mean of Group1 is computed by taking each value of x. The intensity is multiplied by the corresponding probability value of the intensity and divided by the normalization. The same thing is done for Group 2. The midpoint between the two mean is then computed. Then the program breaks out if there is no further changes. Each image has 3 dimensions, the length, width, and RGB values. From the fluorescent image of Figure 23, we determine the threshold value of green, representing fluorescent active region, by global thresholding algorithm computation. This would help us to filter into a binary image, as shown in Figure 27. The images can also be further filtered by edge detection by MATLAB function bwmorph(a, 'dilate', 5), which dilates the image 5 times to include pixels at the edge. Finally, we select points in the active region by creating matrix of RGB values, as shown in Figure 28. Figure 29 shows the pixel intensity of PANI, PANI+probe, and PANI+duplex based on extracting the RGV values of the green active region of the image. The result clearly correlates the fluorescence data we previously got based on quantitative value of average pixel intensity.

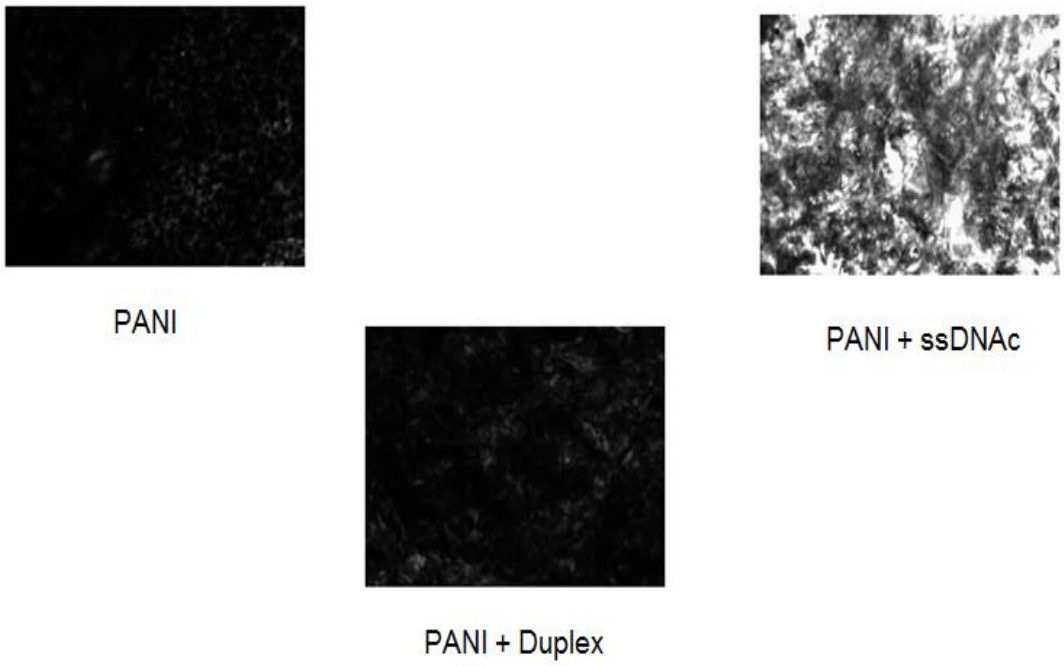

Figure 27. Binary image of fluorescence after color thresholding

The object selection can be done by threshold-based counting in an Image Pro Plus software. Here, the first thing we do is select our object based on the color threshold which has been computed. The outline of the object as well as a dot for filled object can be counted. If there is thresholding error, we do edge correction by filling holes. We also can measure any properties other than pixel intensity like mean intensity, diameter, perimeter, roundness, size of length etc. Finally, when measurement data is viewed, we get a table that shows every single object and all those data we have requested for measurement.

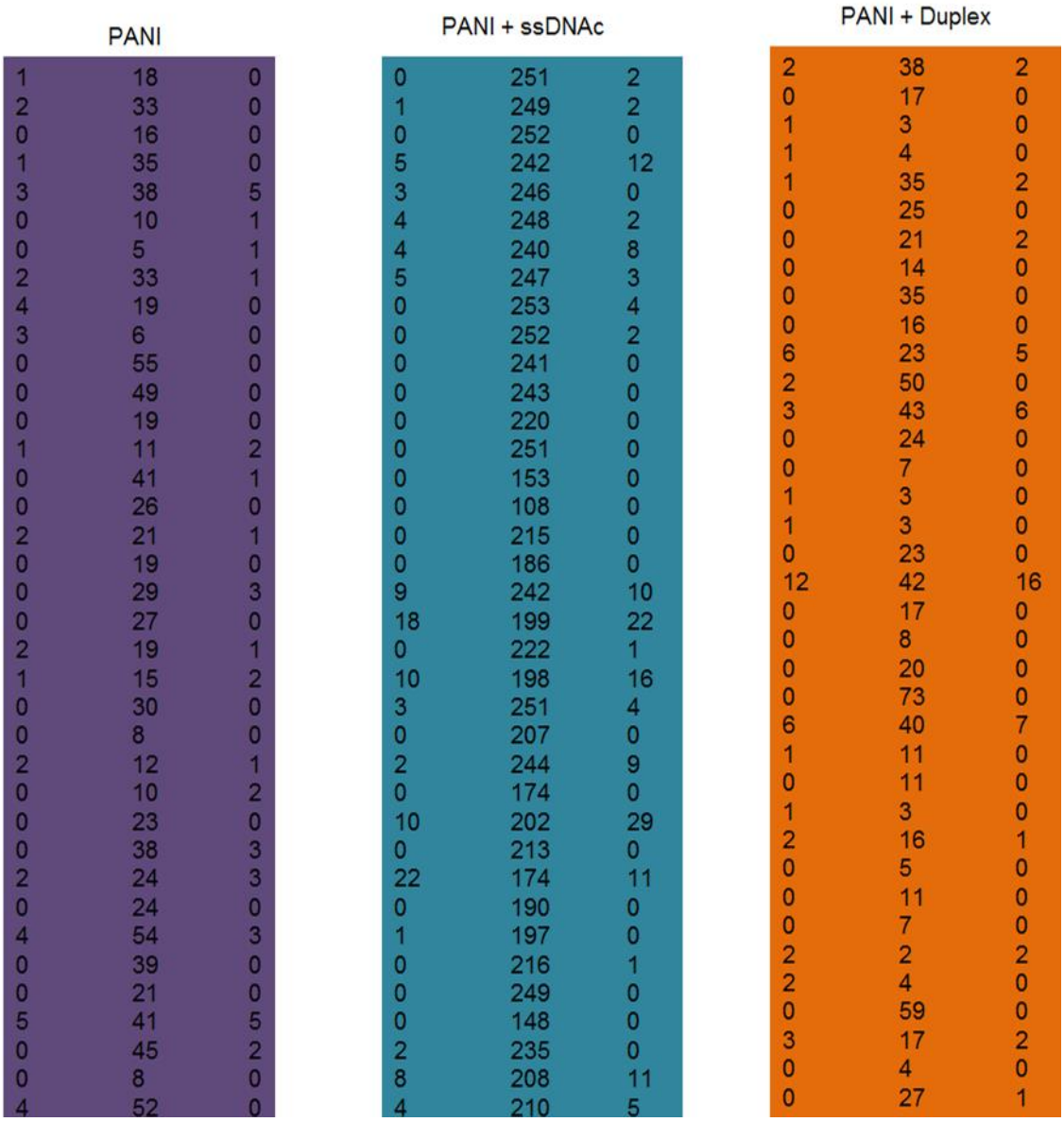

PANI		
1	18	0
2	33	0
0	16	0
1	35	0
3	38	5
0	10	1
0	5	1
2	33	1
4	19	0
3	6	0
0	55	0
0	49	0
0	19	0
1	11	2
0	41	1
0	26	0
2	21	1
0	19	0
0	29	3
0	27	0
2	19	1
1	15	2
0	30	0
0	8	0
2	12	1
0	10	2
0	23	0
0	38	3
2	24	3
0	24	0
4	54	3
0	39	0
0	21	0
5	41	5
0	45	2
0	8	0
4	52	0

PANI + ssDNAc		
0	251	2
1	249	2
0	252	0
5	242	12
3	246	0
4	248	2
4	240	8
5	247	3
0	253	4
0	252	2
0	241	0
0	243	0
0	220	0
0	251	0
0	153	0
0	108	0
0	215	0
0	186	0
9	242	10
18	199	22
0	222	1
10	198	16
3	251	4
0	207	0
2	244	9
0	174	0
10	202	29
0	213	0
22	174	11
0	190	0
1	197	0
0	216	1
0	249	0
0	148	0
2	235	0
8	208	11
4	210	5

PANI + Duplex		
2	38	2
0	17	0
1	3	0
1	4	0
1	35	2
0	25	0
0	21	2
0	14	0
0	35	0
0	16	0
6	23	5
2	50	0
3	43	6
0	24	0
0	7	0
1	3	0
1	3	0
0	23	0
12	42	16
0	17	0
0	8	0
0	20	0
0	73	0
6	40	7
1	11	0
0	11	0
1	3	0
2	16	1
0	5	0
0	11	0
0	7	0
2	2	2
2	4	0
0	59	0
3	17	2
0	4	0
0	27	1

Figure 28. Pixel value after color thresholding by MATLAB

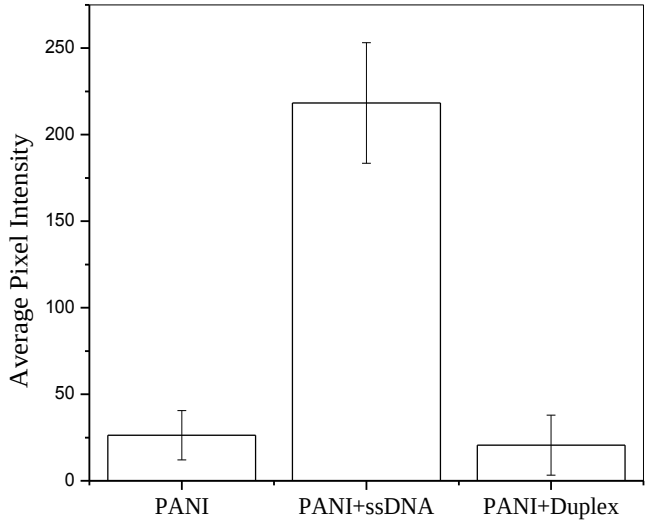

Figure 29. Average pixel intensity of PANI, PANI+probe and PANI-Duplex

Conclusions

This research work is conducted to develop a uniform coating based on tuning of the surface energy of borosilicate glass and the surface energy of PANI coating. For this, we reduce contact angle of hydrophobic glass surface by treatment with UV/H_2O irradiation and, at the same time, make PANI more hydrophobic by encapsulating it with PEG. The fluorescence image of PANI coating was segmented using color thresholding by computing threshold intensity by global threshold algorithm and iterating it with a MATLAB program. Finally, using the threshold, the active part of the image is segmented, and pixel intensity is calculated which correlates well with our previous fluorescence intensity measurement of PANI, PANI immobilized and PANI duplex.

CHAPTER IV

SUMMARY AND CONCLUSION

In this research work, we are able to develop a sensor, which has better attributes than existing micro RNA analysis methods. Our fluorescent-based sensor platform performs a rapid and sensitive identification of micro RNA or mimic DNA molecules within 15 minutes of interaction and also at a very low concentration of 10 pM of target oligonucleotide. Profiling micro RNA is a challenging task, given that standard methods currently used like Northern blotting, *in situ* hybridization, deep sequencing, microarrays and reverse transcript PCR methods fail to quantitatively map micro RNA in clinical samples. Commonly used methods like Northern Blotting and *in-situ* hybridization have poor sensitivity and are time consuming. They also fail in point of care application. Our sensor platform is found to be very selective and shows significant difference in fluorescence property for one base mismatch target oligonucleotide. Our developed sensor also addresses a key issue to distinguish and differentiate precursor and mature state micro RNAs since the mature micro RNA is active in cellular development, while precursors does not necessarily correspond to cellular concentration of functional micro RNAs. Another important novelty of our sensor is the oligo probe is that immobilized by electrostatic interaction with the PANI platform, while in most literature reports, the current technology indicates covalent attachment. The electrostatic attachment renders high sensitivity and conformational flexibility of our sensor in presence of target oligonucleotide environment.

In this research, we are able to develop nucleic acid-based sensor on PANI platform and UV assisted immobilized probes. This research aims to create a strategy

based on electrostatic immobilization of probe oligos on PANI that was enhanced by UV irradiation. Thus, PANI-based sensor platform would be able to detect hybridization of oligos complimentary to probes with great specificity, and distinguish between perfectly complementary oligos and one only having a single mismatch. The platform would also have high sensitivity and would be capable of detecting amounts of target oligo by using probe-dissociation-based transduction or detection without secondary compounds. The sensor is also robust enough and successfully detects expression of a micro RNA in total RNA extract. This is important as micro RNAs are an enigma of small molecules representing a tiny fraction of total RNA present in the cell. Many of them belong to the same family of few nucleotide mismatches, challenging the specificity and selectivity of sensor response. Another objective is to exclude direct and indirect labeling of micro RNAs. The labeling incurs high cost and also affects stability and sensitivity of the sensor. Our sensor transduces fluorescence as an intrinsic property of PANI. The choice of fluorescence property is made because in the area of bio imaging, fluorescence is one of the principal tools of both in-vitro and vivo cellular observations. Another important achievement of the research is the development of water processable and nanomaterial PANI for signal transduction. The main advantages of nanomaterials are that they have high surface to volume ratio of molecular structure, which largely affects sensitivity and signal transduction. Finally, we opt to create a combined fluorescence microscopy technique and signal processing methods as a powerful tool for cell analysis. The amalgamation of sensor response with robust image analysis would pave the path for a biochip technology that would help monitor multiple genes at a time with fast computing speed and small volumes of clinical samples. The ongoing research is based on

developing a uniform coating and taking 2D fluorescence image at different concentration of probe and complementary concentration of ssDNA *let-7* mimic, and micro RNA. The focus of the research work is to undergo image segmentation using MATLAB. Image segmentation involves development of algorithm to find appropriate thresholding for segmenting the fluorescence and also combination of dilation-erosion (Openings and Closings) operations to get better image analysis. Future direction of research would be to identify micro RNA population and specific cluster image identification of analysis from a population of micro RNA say, blood serum transducing fluorescent signal from PANI based probe array. Fluorescence in bio imaging is extensively used because it helps in micron range observation of detailed activities. Fluorescence spectroscopy can also independently detect cellular activity without much interference, if efficient segmentation of signal is achieved. Thus, with this technology, we would be able to capture and convert the chemistry of genetic diseases while decoding and monitoring micro RNAs, DNA, and proteins and relations between them so that diseases can be detected early and therefore, can be prevented. Our future work aims to explore other CPs, such as PPy, PTh, and copolymers as transduction matrix element. Currently, we are also exploring bridgehead imine substituted cyclopentadithiophene structural units of low and tunable band gap donor-acceptor polymers, which allow us to modify the electronic properties of the polymers with unprecedented precision. A multiplex sensor array involving these polymers would facilitate detection of a population of micro RNA by their signature optoelectronic properties. This would leverage the research work to the development of the final goal of a biochip developed for fast detection of each of specific micro RNAs from a population.

APPENDIX

RELATED PUBLICATIONS

BioMACROMOLECULES

Article

pubs.acs.org/Biomac

Utilizing Intrinsic Properties of Polyaniline to Detect Nucleic Acid Hybridization through UV-Enhanced Electrostatic Interaction

Partha Pratim Sengupta,[†] Jared N. Gloria,[†] Dahlia N. Amato,[‡] Douglas V. Amato,[‡] Derek L. Patton,[‡] Beddhu Murali,[§] and Alex S. Flynt*[,†]

[†]Department of Biological Sciences, [‡]School of Polymers and High Performance Materials, and [§]School of Computing, University of Southern Mississippi, Hattiesburg, Mississippi 39406, United States

ABSTRACT: Detection of specific RNA or DNA molecules by hybridization to "probe" nucleic acids via complementary base-pairing is a powerful method for analysis of biological systems. Here we describe a strategy for transducing hybridization events through modulating intrinsic properties of the electroconductive polymer polyaniline (PANI). When DNA-based probes electrostatically interact with PANI, its fluorescence properties are increased, a phenomenon that can be enhanced by UV irradiation. Hybridization of target nucleic acids results in dissociation of probes causing PANI fluorescence to return to basal levels. By monitoring restoration of base PANI fluorescence as little as 10^{-11} M (10 pM) of target oligonucleotides could be detected within 15 min of hybridization. Detection of complementary oligos was specific, with introduction of a single mismatch failing to form a target−probe duplex that would dissociate from PANI. Furthermore, this approach is robust and is capable of detecting specific RNAs in extracts from animals. This sensor system improves on previously reported strategies by transducing highly specific probe dissociation events through intrinsic properties of a conducting polymer without the need for additional labels.

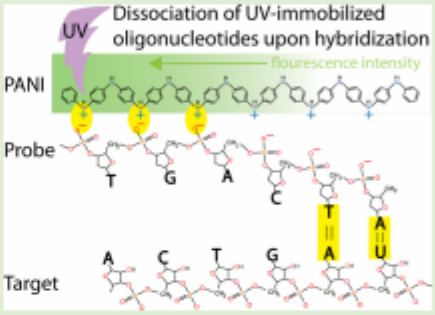

INTRODUCTION

Electroconductive polymers (CPs) have many applications in electronic devices and molecular sensors.[1−7] In biosensors, a promising use of CPs is in the sensing of nucleic acids: a versatile strategy for characterizing cells and their behaviors.[8,9] Indeed, detection of RNA and DNA is frequently a component of diagnostic technologies used in the clinic and biological research. One of the most common methods of detecting a specific RNA or DNA involves hybridization of probes through complementary base-pairing. This strategy is the basis of venerable southern/northern blotting methods and microarray technology.[10]

There are many reports of incorporating different CP chemistries into hybridization-based RNA/DNA sensors that are similar to microarray technology where probes are covalently attached or entrapped in CP matrics.[11−16] In these formats, electrical and fluorescence properties of CPs have been used to transduce hybridization events, though in many cases secondary detection with electroactive compounds or fluorescent moieties is necessary.[12,17−23] This strategy has some limitations due to the ability of nucleic acids to spontaneously interact with cationic polyelectrolytes, making it difficult to distinguish bona fide hybridization events from spurious interactions with nontarget DNA or RNA.[24,25] Furthermore, approaches that use permanent association of probes are frequently reported to be unable to distinguish single base-pair mismatches.[12] This unfortunately makes technologies based on these approaches ill-suited to detect single-nucleotide polymorphisms or distinguish other highly related sequences.

Organic polymers also provide opportunities to generate sensor platforms that are distinct from microarrays. A common alternative takes advantage of the formation of electrostatic complexes between polymers and probes oligos that is driven by interactions between polymer cationic groups and phosphate or nitrogenous bases in DNA.[26,27] While many polymers have been tested in electrostatic attachment-based sensors, a common observation is that target hybridization disrupts the attachment of probes with polymer causing dissociation.[28−33] A common strategy to exploit this behavior is to bond a fluorophore-conjugated probe with a polymer that is capable of quenching fluorescence.[34] After hybridization, fluorescence is restored due to dissociation of the probe and subsequent dequenching of the label. Studies using this strategy report high specificity, where even a single base-pair mismatch can be

Received: June 29, 2015
Revised: September 11, 2015
Published: September 21, 2015

DOI: 10.1021/acs.biomac.5b00935
Biomacromolecules 2015, 16, 3217−3225

REFERENCES

Abdolahi, A., Hamzah, E., Ibrahim, Z., & Hashim, S. (2012). Synthesis of Uniform Polyaniline Nanofibers Through Interfacial Polymerization. *Materials*, *5*(8), 1487-94.

Abubakar, F.M. (2012). A Study of Region-Based and Contour Based Image Segmentation. *Signal & Image Processing, 3*(6), 15-22.

Abu-Salah, K., Zourob, M., Mouffouk, F., Alrokayan, S.A., Alaamery, M.A., & Ansari, A.A. (2015). DNA Based Nanobiosensors as an Emerging Platform for Detection Of Disease. *Sensors (Basel)*, *15*(6), 14539-68.

Adessi, C., Matton, G., Ayala, G., Turcatti, G., Mermod, J.J., Mayer, P., & Kawashima, E. (2000). Solid Phase DNA Amplification: Characterization of Primer Attachment and Amplification Mechanisms. *Nucleic Acids Research*, *28*(20), e87.

Ahuja, T., Mir, I.A., Kumar, D., & Rajesh,. (2007). Biomolecular Immobilization on Conducting Polymers for Biosensing Applications. *Biomaterials*, *28*(5), 791-805.

Algeciras-Schimnich, A., Pietras, E.M., Barnhart, B.C., Legembre, P., Vijayan, S., Holbeck, S.L., & Peter, M.E. (2003). Two CD95 Tumor Classes with Different Sensitivities to Antitumor Drugs. *Proceedings of the National Academy of Sciences*, *100*(20), 11445-50.

Ates, M. (2013). A Review Study of (Bio)sensor Systems Based on Conducting Polymers. *Materials Science and Engineering: C, 33*(4), 1853-59.

Ates, M., Karazehir, T., & Sarac, A.S. (2012). Conducting Polymer Nanomaterials. *Nanomaterials*, *3*(3), 524-49.

Bai, H. & Shi, G. (2007). Gas Sensors Based on Conducting Polymers. *Sensors, 7,* 267-307.

Bal Sydulu, S., Palamappan, S., & Srinivas, P. (2003). Nanofibre Polyaniline Containing Long Chain and Small Molecule Dopants and Carbon Composites for Supercapacitor. *Electrochimica Acta*, *95,* 251-59.

Bammler, T., Beyer, R.P., Bhattacharya, S., Boorman, G.A., Boyles, A., Bardford, B.U., Bumgarner, R.E., Bushel, P.R., Chaturvedi, K., Choi, D., Cuningham, M.L., Deng, S., Dressman, H.K., Fanin, R.D., Farin, F.M., Freedman, J.H., Fry, R.C., Harper, A., Humble, M.C., Hurban, O., Kavanagh, T.J., Kaufmann, W.K., Kerr, K.F., Jing, L., Lapidus, J.A., Lasarer, M.R., Li, J., Li, Y.J., Lobenhofer, E.K., Lu, X., Malek, R.L., Milton, S., Nagalla, S.R., Omalley, J.P., Palmer, V.S., Paltee, P., Paules, R.S., Perous, C.M., Philips, K., Qin, L.X., Qiu, Y., Quigley, S.D., Rodland, M., Rusyn,I., Samson, L.D., Schwartz, D.A., Shi, Y., Shin, J.L., Sieber, S.D., Slifer, S., Speer, M.C., Spencer, P.S., Sproles, D.I., Swenberg, J.A., Suk, W.A., Sullivan, R.C., Tian, R., Tennant, R.W., Todd, S.A., Tucker, C.J., Van Houten, B., Weis, B.K., Xuan, S., Zarbi, H., & Members of the Toxicogenomics Rsearch Consortium (2005). Standardizing Global Gene Expression Analysis Between Laboratories and Across Platforms. *Nature Methods*, *2*(50, 351-56.

Bartel, D.P. (2004). Micro RNAs: Genomics, Biogenesis, Mechanism, and Function. *Cell*, *116*(2), 281-97.

Blount, K.F., & Tor, Y. (2003). Using Pyrene-Labeled HIV-1 TAR to Measure RNA-Small Molecule Binding. *Nucleic Acids Research*, *31*(19), 5490-5500.

Boyerinas, B., Park, S.M., Hau, A., Murmann, A.E., & Peter, M.E. (2010). The Role of Let-7 in Cell Differentiation and Cancer. *Endocrine Related Cancer*, *7(*1), 19-36.

Bowman, C.L. (1998). Quantifying the Cleanliness of Glass Capillaries. *Cell Biochemistry and Biophysics*, *29*(3), 203-23.

Buxboim, A., Bar-Dagan, M., Frydman, V., Zbaida, D., Morpurgo, M., & Bar-Ziv, R. (2007). A Single-Step Photolithographic Interface for Cell-Free Gene Expression and Active Biochips. *Small*, *3*(3), 500-10.

Carthew, R.W., & Sontheimer, E.J. (2009). Origins and Mechanisms of MiRNAs and SiRNAs. *Cell*, *136*(4), 642-55.

Cosnier, S. (1999). Biomolecule Immobilization on Electrode Surfacesby Entrapment or Attachment to Electrochemically Polymerized Films. A Review. *Biosensors and Bioelectronics*, *14*(5), 443-56.

Chen, S., Li, L., Zhao, C., & Zheng, J. (2010). Surface Hydration: Principles and Applications Toward Low Fouling/Nonfouling Biomaterials. *Polymer*, *51*(3), 5283-93.

Chen, X., Guo, Z., Yang, G.M., Li, J., Li, M.Q., Liu, J.H., & Hunag, X.-J. (2010). Electrical Nanogap Devices for Biosensing. *Materials Today*, *13*(11), 28-41.

Cheng, S.F., Li, L. & Wang, L.M. (2015). MiR-155 and MiR-146b Negatively Regulates IL6 in Helicobacter Pyroli (Cag A+) Infected Gastroduodenal Ulcer. *European Review For Medical And Pharmocological Sciences*, *19*(4), 607-13.

Darling, S.B. (2008). Isolating the Effect of Torsional Defects on Mobility and Band Gap in Conjugated Polymers. *The Journal of Physical Chemsitry B*, *112*(30), 8891-95.

Debnath, M., Prasad, G.B.K.S., & Bisen, P.S. (2010). Molecular Diagnostics: Promises and Possibilities. NewYork: Springer.

DeRosa, R.L., Schader, P.A., & Shelby, J.E. (2003). Hydrophilic Nature of Silicate Glass Surfaces as a Function of Exposure Condition. *Journal of Non-Crystalline Solids, 331*, 32-40.

Dima, A.A., Elliott, J.T., Filliben, j.J., Halter, M., Peskin, A., Bernal, J., Kociolek, M., Brady, M.C., Tang, H.C., & Plant, A.L. (2011). Comparison of Segmentation Algorithms for fluorescence Microscopy Images of Cells. *Cytometry Part A*, *79A*, 545-59.

Efimenko, K., Wallace, W.E., & Genzer, J. (2002). Surface Modification of Sylgard-184 Poly(Dimethylsiloxane) Networks by Ultraviolet And Ultraviolet/Ozone Treatment. *Journal of Colloid and Interface Science*, *254*, 306-15.

Ekimler, S., & Sahin, K. (2014). Computational Methods for Micro RNA Target Prediction. *Genes (Basel)*, *5(*3), 671-83.

Escoubas, L., Gatto, A., Albrand, G., Roche, P., & Commandre, M. (1998). Solarization of Glass Substrates During Thin-Film Deposition. *Applied Optics*, *37*(10), 1883-89.

Falcao, E.H.L., & Azevedo, W.M. de. (2002). Polyaniline-Poly(Vinyl Alcohol) Composite as an Optical Recording material. *Synthetic Metals*, *128*, 149-54.

Faure, B., Salazar-Alvarez, G., Ahniyaz, A., Villaluenga, I., Berriozabal, G., Miguel, Y.R.D., & Bergstrom, L. (2013). Dispersion and Surface Functionalization of Oxide nanoparticles for Transparent Photocatalytic and UV-protecting Coatings and Sunscreens. *Science and Technology of Advanced Materials*, *14*, 023001.

Feldman, K.E., & Martin, D.C. (2012). Functional Conducting Polymers via Thiol-ene Chemistry. *Biosensors*, *2*(3), 305-17.

Fouad, I., Mabrouk, M., & Sharawy, A. (2014). Automatic Segmentation of cDNA Microarray Images Using Different Methods. *Journal of Biomedical Engineering and Medical Imaging*, *1*(5), 42-52.

Friedman, R.C., Farh, K.K.H., Burge, C.B., & Bartel, D.P. (2009). Most Mammalian mRNAs are Cinsidered Targets of Micro RNAs. *Genome Research*, *19*(1), 92-105.

Garzon, R., Marcucci, G., & Croce, C.M. (2010). Targeting Micro RNAs in Cancer Rationale, Strategies and Challenges. *Nature Reviews Drug Discovery*, *9*(10), 775-89.

Gawel, K., Barriet, O., Sletmoen, M., & Torger-Stokke (2010). Responsive Hydrogels for Label Free Signal Transduction Within Biosensors. *Sensors*, *10*, 4381-4409.

Gaylord, B.S., Heeger, A.J., & Bazan, G.C. (2003). Hybridization Detection with Water-Soluble Conjugated Polymers and Chromophore-Labeled Single Stranded DNA. *Journal of the American Chemical Society*, *125*(4), 896-900.

Gerard, M., Chaubey, A., & Malhotra, B.D. (2002). Application of Conducting Polymers to Biosensors. *Biosenors and Bioelectronics*, *17*, 345-59.

Ha, T.Y. (2011). Micro RNAs in Human Diseases: From Cancer to Cardiovascular Disease. *Immune Network*, *11*(3), 135-54.

Hahm, J. (2011). Functional Polymers in Protein Detection Platforms: Optical, Electrochemical, Electrical, Mass Sensitive, and Magnetic Biosensors, *Sensors (Basel)*, *11*(3), 3327-55.

Han, Y.G., Kusunose, T., Sekino, T. (2009). One Step Reverse Micelle Polymerization of Organic Dispersible Polyaniline Nanoparticles, *Synthetic Metals*, *159*(1-2), 123-131.

Henry, N.L. & Hayes, D.F. (2012). Cancer Biomarkers. *Molecular Oncology*, *6*(2), 140-46.

Hu, J., Zhu, Z., Zheng, Y., Xiong, W., & Ding, Y. (20140. Characterization of conserved Micro RNAs from Five Different Cucurbit Species Using Computational and Experimental Analysis. *Biochimie*, *102*, 137-44.

Huang, T., Yang, J., Liu, G., Jin, W., Liu, Z., Zhao, S., & Yao, M. (2015). Quantification of Mature Micro RNAs Using Primer Probes and Real Time PCR Amplification. *PLoS One*, *10*(3), e0120160.

Iorio, M.V., & Croce, C.M. (2012). Micro RNA Dysregulation in Cancer: Diagnostics, Monitoring and Therapeutics. A Comprehensive Review. *EMBO Molecular Medicine*, *4*(3), 143-59.

Janata, J., & Josowicz, M. (2003). Conducting Polymers in Electronic Chemical Sensors. *Nature Materials*, *2*, 19-24.

Johnson, S.M., Grosshans, H., Shingara, J., Byrom, M., Jarvis, R., Cheng, A., Labourier, E., Reinert, K.L., Brown, D., Cheng, A., Labourier, E., Reiner, K.L., Brown, D., & Slack, F.J. (2005). RAS is Regulated by the Let-7 Micro RNA Family. *Cell*, *20*(5), 635-47.

Jia, W., Kornemandel, D., Lamhot, Y., Narkis, M., & Siegmann, A. (2002). Polyaniline-DBSA/Organophilic Clay Nanocomposites: Synthesis and Characterization. *Synthetic Metals*, *128*(1), 115-120.

Kadashchuk, A., Arkhipov, V.I., Kim, C.H., Shinar, J., Lee, D.W., Hong, Y.R., Jin, J.II, Heremans, P., & Bassler, H. Localized Trions in Conjugated Polymers. *Physical Reviews B*, *76*, 235205.

Kar, P. (2013). Doping in Conjugated Polymers, Beverly, MA: Scrivener Publishing.

Kerppola, T.K. (2008). Bimolecular Fluorescence Complementation (BiFC) Analysis as a Probe of Protein Interactions in Living Cells. *Annual Review of Biophysics*, *37*, 465-87.

Khandekar, V.S., & Samani, K.A. (2014). A Brief Review of Segmentation Methods for Medical Images. *International Journal of Research in Engineering and Technology*, *3*(1), 421-27.

Khrapko, R., Lai, C., Casey, J., Wood, W.A., & Borrelli, N.F. (2014). Accumulated Self-Focussing of Ultraviolet Light in Silica Glass. *Applied Physics Letters*, *105*, 244110.

Kim, B.J., Oh, S.G., Han, M.G., & Im, S.S. (2001). Synthesis and Characterization of Polyaniline Nanoparticles in SDS Micellar Solutions. *Synthetic Metals*, *122*(2), 297-304.

Kircheis, R., Blessing, T., Brunner, S., Wightman, L., & Wagner, E. (2001). Tumor Targeting with Surface-Shielded Ligand Polycation DNA Complexes. *Journal of Controlled Release*, *72*(1-3), 165-70.

Koshkin, A.A., Singh, S.K., Nielsen, P., Rajwanshi, V.K., Kumar, R., Meldgaard, M., Otsen, C.E., & Wenger, J. (1998). LNA (Locked Nucleic Acids): Synthesis of the Adenine, Cytosine, Guanine, 5-Methyl Cytosine, Thymine and Uracil

Bicyclonucleoside Monomers, Oligomerisation, and Unprecedented Nucleic Acid Recognition. *Tetrahedron, 54*(14), 3607-30.

Kwon, M.J., & Shin, Y.K. (2011). Epigenetic Regulation of Cancer Associated Genes in Ovarian Cancer. *International Journal of Molecular Sciences, 12*(2), 983-1008.

Lee, Y.S., & Dutta, A. (2007). The Tumor Suppressor Micro RNA Let-7 Represses the HMGA2 Oncogene. *Genes & Development, 21*(9), 1025-30.

Lee, J.H., Jang, A., Bhadri, P.R., Myers, R.R., Timmons, W., Beyette, Jr F.R., Bishop, P.L., & Papantsky, I. (2006). Fabrication of Microelectrode Arrays For In Situ Sensing of Oxidation Reduction Potentials, *Sensors and Actuators B, 115*, 220-226.

Liu, J., Tian, S., Tiefenauer, L., Nielsen, P.E., & Knoll, W. (2005). Simultaneously Amplified Electrochemical and Surface Plasmon Optical Detection of DNA Hybridization Based on Ferrocene Streptavidin Conjugates. *Analytical Chemistry, 77*(9), 2756-61.

Lodish, H., Berk, A., Zipursky, S.L., Matsudaira, P., Baltimore, D., & Darnell, J. (2000). Molecular Cell Biology, NewYork: W.H. Freeman.

Lou, X., He, P., Okelo, G.O., & He, L. (2006). Radical Polymerization In Biosensing. *Analytical and Bioanalytical Chemistry*, 386, 525-31.

MacFurlane, L.A. & Murphy, P.R. (2010). Micro RNA: Biogenesis, Function and Role in Cancer. *Current Genomics, 11*(7), 537-61.

Mathieu, J., & Ruohola-Baker, H. (2013). Regulation of Stem Cell Populations by Micro RNAs. *Advances in Experimental Medicine and Biology, 786*, 329-51.

Mestdagh, P., Hartmann, N., Baeriswyl, L., Andreasen, D., Bernard, N., Chen, C., Cheo, D., D'Andrade, P., DeMayo, M., Dennis, L., Derveawx, S., Feng, Y., Fulmer-Smentek, S., Gerstmayer, B., Gouffon, J., Grimley, C., Lader, E., Lee, K.Y., Lue, S., Peiffer, S., Ruberg, S., & Schroth, G. (2014). Evaluation of Quatitative MiRNA Expression Paltforms in the Micro RNA Quality Control (MiRQC) Study. *Nature Methods*, *11*, 809-15.

Namgoong, H., Woo, D.J., & Lee, S.H. (2007). Micro-Chemical Structure of Polyaniline Synthesized by Self Stabilized Dispersion Polymerization. *Macromolecular Research*, *15*(7), 633-39.

Noriega, R., Rivnay, J., Vandewal, K., Koch, F.P.V., Stingelin, N., Smith, P., Toney, M.F. & Salleo, A. (2013). A General Relationship Between Disorder, Aggregation and Charge Transport in Conjugated Polymers. *Nature Materials*, 12, 1038-44.

Owen, D.M., Williamson, D.J., Boelen, L., Magenau, A., Rossy, J., & Gaus, K. (2013). Quantitative Analysis of Three-Dimensional Fluorescence Localization Microscopy Data. *Biophysical Journal*, *105*(2), 205-07.

Owen, D.M., Williamson, D., Magenau, A., Rossy, J., & Gaus, K. (2012). Optical Techniques for Imaging Membrane Domains in Live Cells (Live-Cell Palm of Protein Clustering). *Methods in Enzymology*, *504*, 221-35.

Pak, T.R., Rao, Y.S., Prins, S.A., & Mott, N.N. (2013). An Emerging Role for Micro RNAs in Sexually Dimorphic Neurobiological Systems. *Pflugers Archiv*, *465*(5), 655-667.

Pan, L., Qiu, H., Dou, C., Li, Y., Pu, L., Xu, J., & Shi, Y. (2010). Conducting Polymer Nanostructures: Template Synthesis and Applications in Energy Storage. *International Journal of Molecular Sciences*, *11*(7), 2636-57.

Park, S.J., Kwon, O.S., Lee, J.E., Jang, J., & Yoon, H. (2014). Conducting Polymer-Based Nanohybrid Transducers: A Political Route to High Sensitivity and Selectivity Sensors, *Sensors (Basel), 14*(2), 3604-30.

Pena, J.T., Sohn-Lee, C., Rouhanifard, S.H., Ludwig, J., Hafner, M., Mihailovic, A., Lim, C., Holoch, D., Berninger, P., Zavoian, M. & Tuschi, T. (2009). MiRNA In Situ Hybridization in Formaldehyde and EDC Fixed Tissues, *Nature Methods*, *6*(2), 139-41.

Peng, H., Zhang, L., Soeller, C., & Travas-Sejdic, J. (2009). Conducting Polymers for Electrochemical DNA Sensing. *Biomaterials*, *30*, 2132-2148.

Peng, H., Soeller, C., Vigar, N., Kilmartin, P.A., Cannell, M.B., Bowmaker, G.A., Cooney, R.P., & Travas-Sejdic, J. (2005). Label-Free Electrochemical DNA Sensor Based on Functionalised Conducting Copolymer. *Biosensor and Bioelectronics*, *20*(9), 1821-28.

Pethe, S.M., & Kondawar, S.B. (2014). Optical And Electrical Properties of Conducting Polyaniline Nanofibers Synthesized by Interfacial and Rapid Mixing Polymerization. *Advanced Materials Letters*, *5*(12), 728-733.

Preat, J., Telxeira-Dias, B., Michaux, C., Perpete, E.A., & Aleman, C. Specific Interactions in Complexes Formed by DNA and Conducting Polymer Building Blocks: Guanine and 3,4-(Ethylenedioxy) Thiophene. *The Journal of Physical Chemistry A*, *115*(46), 13642-48.

Quillen, D.A. (1999). Common Causes of Vision Loss in Elderly Patients. *American Family Physician*, *60*(1), 99-108.

Rahman, M.M., Li, X.B., Lopa, N.S., Ahn, S.J., & Lee, J.J. (2015). Electrochemical DNA Hybridization Sensors Based on Conducting Polymers, *Sensors(Basel)*, *15*(2), 3801-29.

Ranganathan, K., & Sivasankar, V. (2014). Micro-RNAs Biology and Clinical Applications. *Journal of Oral and Maxillofacial Pathology, 18*(2), 229-34.

Rao, P., Benito, E., & Fischer, A. (2013). Micro RNAs as Biomarkers for CNS Disease. *Frontiers in Molecular Neuroscience*. *6*, 39.

Raymond, F.R., Ho, H.A., Peytavi, R., Bissonnette, L., Boissinot, M., Picard, F.J., Leclerc, M., & Bergeron, M.G. (2005). Detection of Target DNA Using Fluorescent Cationic Polymer and Peptide Nucleic Acid Probes on Solid Support. *BMC Biotechnology*, *5*,10.

Ross, D.T., Scerf, U., Eisen, M.B., Perou, C.M., Rees, C., Spellman, P., Iyer, V., Jeffrey, S.S., Vande Rijn, M., Waltham, M., Pergamenschikov, A., Lee, J.C., Lashkari, D., Shalon, D., Myers, T.G., Weinstein, J.N., Botstein, D., & Brown, P.O. (2000). Systematic Variation in Gene Expression Patterns in Human Cancer Cell Lines. *Nature Genetics, 24*(3), 227-35.

Sabirmeeza, A.A.F., & Subhashini, S. (2013). A Novel Water-Soluble Conducting Polymer Composite for Mild Steel Acid Corrosion Inhibition. *Journal of Applied Polymer Science*, *127*(4), 3084-92.

Sadava, D., Hill, R.W., Hillis, D.M., & Price, M.V. (2014). *Principles of Life*. Sunderland, MA: Sinauer Associates, Macmillan.

Salaneck, W.R., Friend, R.H., & Bredas, J.L. (1999) Electronic Structure of Conjugated Polymers: Consequences of Electron-Lattice Coupling. *Physics Reports, 319*(6), 231-51.

Sambasevam, K.P., Mohamad, S., & Phang, S.W. (2015). Enhancement of Polyaniline Properties by Different Polymerization Temperatures in Hydrazine Detection. *Journal of Applied Polymer Science, 132*(13), 1-8.

Sampson, V.B., Rong, N.H., Han, J., Yang, Q., Aris, V., Soteropoulos, P., Petrelli, N.J., Dunn, S.P., & Krueger, L.G. (2007). Micro RNA Let-7a Down Regulates MYC and Reverts MYC-Induced Growth in Burkitt Lymphoma Cells. *Cancer Research, 67*(20), 9762-70.

Santhanam, K.S.V. (1998). Conducting Polymers for Biosensors: Rationale Based on Models. *Pure and Applied Chemistry, 70*(6), 1259-62.

Santiago, E.I., Pereira, E.C., & Bulhoes, L.O.S. (1998). Characterization of the Redox Processes in Polyaniline Using Capacitance-Potential Curves, *Synthetic Metals, 98*(2), 87-93.

Saranya, K., Rameez, M., & Subramania, A. (2015). Developments in Conducting Polymer Based Counter Electrodes for Dye-Sensitized Solar Cells-An Overview. *European Polymer Journal, 66*, 207-27.

Schirwitz, C., Loeffler, F.F., Felgenhauer, T., Stadler, V., Breitling, F., & Bischoff, F.R. (2012). Sensing Immune Responses with Customized Peptide Microarrays. *Biointerphases, 7*(1-4), 47.

Sevignani, C., Calin, G.A., Siracusa, L.D., & Croce, C.M. (2006). Mammalian micro RNAs: A Small World for Fine-Tuning Gene Expression. *Mammalian Genome, 17*(3), 189-202.

Shapiro, L.G., & Stockman, G. (2001). *Computer Vision*. Upper Saddle River, NJ:, Prentice-Hall.

Sharma, P., Modi, S.R., & Bansal, A.K. (2015). Co-processing of Hydroxyl Propyl Methyl Cellulose (HPMC) for Improved Aqueous Dispensibility. *International Journal of Pharmaceutics, 485*, 348-56.

Shell, S., Park, S.M., Radjabi, A.R., Schickel, R., Kistner, E.O., Jewell, D.A., Feig, C., Lengyel, E., & Peter, M.E. (2007). Let-7 Expression Defines Two Differentiation Stages of Cancer. *Proceedings of the National Academy of Sciences of the United States of America, 104*(27), 11400-05.

Shi, X., Zhou, W., Ma, D., Ma, Q., Bridges, D., Ma, Y., & Hu, A. (2015). Electrospinning of Nanofibers and Their Applications For Energy Devices. *Journal of Nanomaterials, 140716*, 1-20.

Singh, K.K., & Singh, A. (2010). A Study of Region Based and Contour Based Image Segmentation. *Signal & Image Processing, 3*(6), 15-22.

Singh, S., & Datar, A. (2013). Edge Detection Techniques Using Hough Transform. *International Journal Of Emerging Technology And Advanced Engineering, 3*(6), 333-37.

Skotheim, T.A., Elsenbaumer, R.L., & Reynolds, J.R. (Eds.). (1998). Handbook of Conducting Polymer, NewYork: Marcel Dekker.

Song, E., & Choi, J.W. (2013). Conductive Polyaniline Nanowire and Its Applications In Chemiresistive Sensing. *Nanomaterials, 3,* 498-523.

Star, A., Tu, E., Niemann, J., Gabriel, J.C.P., Joiner, C.S. & Valcke, C. (2006). Label-Free Detection of DNA Hybridization Using Carbon Nanotube Network Field-Effect Transistors. *Proceedings of the National Academy of Sciences*, *103*(4), 921-26.

Stefani, G., Chen, X., Zhao, H., & Slack, F.J. (2015). A Novel Mechanism of Lin-28 Regulation of Let-7 Micro RNA Expression Revealed By in Vitro HITS-CLIP in C.Elegans. *RNA*, *21*(5), 985-96.

Thamizhvanan, K., Kumuda, P., & Nandakishore, R. (2012). A Brief Review on Microarrays. *Journal of Science*, *2*(2), 81-90.

Travas-Sejdic, J., Aydemir, N., Kannan, B., Williams, D.E., & Malmstrom, J. (2013). Intrinsically Conducting Polymer Nanowires for Biosensing. *Journal of Materials Chemsitry B*, *2*, 4593-4609.

Tsotcheva, D., Tsanov, T., Terlemezyan, L., & Vassilev, S. (2001). Structural Investigations of Polyaniline Prepared in the Presence of Dodecylbenzenesulfonic Acid. *Journal of Thermal Analysis and Calorimetry*, *63*, 133-141.

Velusamy, V., Arshak, K., Yang, C.F., Yu, Lei, Korostynska, O. & Adley, C. (2011). Comparison Between DNA Immobilization Techniques on a Redox Polymer Matrix, *American Journal of Analytical Chemsitry*, *2*, 392-400.

Wanekaya, A.K., Chen, W., Myung, N.V., & Mulchandani, A. (2006). Nanowire-Based Electrochemical Biosensors. *Electroanalysis, 18*(6), 533-50.

Wolfbeis, O.S. (2015). An Overview of Nanoparticles Commonly Used in Fluorescent Bioimaging, *Chemical Society Reviews, 44*, 4743-68.

Wolfert, M.A., Dash , P.R., Nazarova, O., Dupicky, D., Seymour, L.W., Smart, S., Strohalm, J. & Ulbrich, K. (1999). Polyelectrolyte Vectors for Gene Delivery: Influence Of Cationic Polymers on biophysical Properties of Complexes Formed With DNA. *Bioconjugate Chemsitry*, *10*(6), 993-1004.

Xu, W., Lucas, A.S., Wang, Z., & Liu, Y. (2014). Identifying Micro RNA Targets in Different Gene Regions. *BMC Bioinformatics*, *15*(7), S4.

Yang, J., Ding, Y., Chen, G., & Li, C. (2007). Synthesis of Conducting Polyaniline Using Novel Anionic Gemini Surfactant As Micellar Stabilizer. *European Polymer Journal*, *43*(8), 3337-43.

Yoon, H. (2013). Current Trends in Sensors Based on Conducting Polymer Nanomaterials. *Nanomaterials*, *3*(3), 524-549.

Yu, H., Chong, Z.Z., Tor, S.B., Liu, E., & Loh, N.H. (2015). Low Temperature And Deformation Free Bonding Of PMMA Microfluidic Devices with Stable Hydrphobicity via Oxygen Plasma Treatment and PVA Coating. *RSC Advances*, *5*, 8377-88.

Zhao, Z., Zhao, Q., Warrick, J., Lockwood, C.M., Woodworth, A., Moley, K.H., & Gronowski, A.M. (2012). Circulating MiR-323-3p as a Biomarker of Ectopic Pregnancy. *Clinical Chemsitry*, *58*(5), 896-905.

Zhang, G.-J., Chua, J.H., Chee, R.E., Agarwal, A. & Wong, S.M. (2009). Label-Free Direct Detection of MiRNAs with Silicon Nanowire Biosensors. *Biosensors and Bioelectronics*, *24*, 2504-08.

Zhang, Y., Zeng, G.M., Tang, L., Li, Y.P., Chen, L.J., Pang, Y., Li, Z., Feng, C.L., & Huang, G.H. (2011a). An Electrochemical DNA Sensor Based on a Layers-Film Construction Modified Electrode. *Analyst*, *136*, 4204-10.

Zhang, Y., Li, H., Luo, Y., Shi, X., Tian, J. & Sun, X. (2011b). Poly (m-Phenylene Diamine) Nanospheres and Nanorods: Selective Synthesis and Their Applications for Multiplex Nucleic Acid Detection. *PLoS ONE*, *6*(6), e20569.

Zhu, J., & Merchant, R.E. (2012). Design Properties of Hydrogel Tissue Engineering Sacffolds. *Expert Review of Medical Devices*, *8*(5), 607-26.